frontiers in Soil Science

TYPE Original Research
PUBLISHED 04 June 2026
DOI 10.3389/fsoil.2026.1789869

OPEN ACCESS

EDITED BY
Jose Navarro Pedreño,
Miguel Hernández University of Elche,
Spain

REVIEWED BY
Julius Incillo Jimenez,
Mariano Marcos State University,
Philippines
Nawel Benouara,
University of Annaba, Algeria

*CORRESPONDENCE
Russell Poma-Chamana
rpomac7@gmail.com

RECEIVED 17 January 2026
REVISED 24 April 2026
ACCEPTED 20 May 2026
PUBLISHED 04 June 2026

CITATION
Poma-Chamana R, Vilca-Gamarra C, Cama-Moreno E and Gómez-Campos P (2026) The drip irrigation paradox in an arid irrigated system: a soil quality index reveals secondary salinization and nutrient accumulation in Southern Peru. *Front. Soil Sci.* 6:1789869. doi: 10.3389/fsoil.2026.1789869

The drip irrigation paradox in an arid irrigated system: a soil quality index reveals secondary salinization and nutrient accumulation in Southern Peru

Russell Poma-Chamana*, Cesar Vilca-Gamarra, Elick Cama-Moreno and Pilar Gómez-Campos

Dirección de Servicios Estratégicos Agrarios, Estación Experimental Agraria de Arequipa, Instituto Nacional de Innovación Agraria (INIA), Calle Saco Oliveros N° 402 - Cerro July, Arequipa, Arequipa, Peru

In arid regions, the conversion of deserts into agricultural land through irrigation is critical for food security but may intensify soil salinization processes. In this context, integrated and spatial soil quality assessment is essential for guiding sustainable management strategies. In this study, we developed a spatially explicit weighted Soil Quality Index (SQIw) and evaluated the effects of irrigation system (drip vs. surface) on soil salinity and fertility within an emerging irrigation scheme in the Peruvian coastal desert. A total of 930 composite soil samples (0–20 cm depth), each composed of 10 subsamples collected within 1-ha parcels, were analyzed for texture, pH, electrical conductivity (EC1:5), organic matter (OM), available phosphorus (Pav), available potassium (Kav), exchangeable sodium (exNa), and carbonates. Principal Component Analysis identified a Minimal Data Set (sand, EC1:5, Kav, OM, pH) explaining 76.8% of the total variance. Indicators were transformed into dimensionless scores (0.1–1.0) using threshold-based scoring functions and weighted according to PCA-derived communalities. Spatial patterns were characterized using semivariogram modeling and Ordinary Kriging, with 10-fold cross-validation confirming unbiased spatial predictions (ME ≈ 0; RMSE = 0.100), though the coefficient of determination remained limited (R^2 = 0.246), consistent with the moderate nugget effects observed across soil properties. The SQIw revealed that 46.7% of the interpolated area fell into the "Poor" category, primarily associated with high salinity areas (EC1:5 > 8 dS m^{-1}) and the predominance of coarse-textured soils, whereas the "Acceptable" category accounted for 53.1% of the evaluated area. Additionally, soils under drip irrigation were associated with significantly higher EC, Kav, and Pav values than surface irrigation, consistent with inadequate leaching fractions, though differences in land development age and management history among sampled fields should be considered when interpreting these results. The SQIw effectively discriminated spatial gradients of soil quality, demonstrating that management-induced improvements remain constrained by inherent edaphic limitations. In naturally saline soils, drip irrigation without specific management practices (e.g., salt leaching) poses a risk of secondary salinization. The proposed methodological framework provides a data-driven tool to support differentiated soil management in arid regions worldwide.

KEYWORDS

arid zones, drip irrigation, geostatistics, ordinary kriging, soil quality index, soil salinity, spatial soil variability

1 Introduction

Soil quality evaluation using integrated indices constitutes an essential tool for diagnosing and sustainably managing agroecosystems, particularly in arid zones where salinization threatens agricultural productivity (1, 2). Soil quality indices (SQI) synthesize multiple indicators into an interpretable metric, facilitating comparisons among assessment methods and additionally supporting more efficient management decisions (3). However, the development of robust SQIs in irrigated saline soils remains challenging due to the pronounced spatial heterogeneity of salinity and fertility-related attributes.

Under arid and semi-arid conditions, particularly in areas with limited natural drainage, soil salts accumulation is favored by the input of salts through irrigation water, the weathering of soils minerals, and decomposition of organic matter. The relative importance of these processes depends on soil type, climate and agricultural management practices (4). Under such conditions, soil salinity shows strong spatial variability driven by differences in groundwater depth, drainage, irrigation system, microtopography, and soil texture (5, 6). This heterogeneity hinders the selection of sensitive indicators and the definition of consistent thresholds, thereby limiting the transferability and robustness of SQIs across management systems (7, 8).

The irrigation system plays a central role in the redistribution of salts and nutrients within the soil profile (9). Despite its high-water use-efficiency, drip irrigation wets a limited soil volume and favors salt accumulations at the margins of the wetted bulb and soil surface, thus requiring periodic leaching to prevent progressive salinization (10, 11). In contrast, surface irrigation methods (flooding, border strips or furrows) generate broader wetting fronts that displace salts to deeper soil layers. This temporarily reduces surface salinity, although reconcentration processes may occur under inadequate management (12). These contrasting mechanisms contribute to the development of differentiated spatial patterns of soil salinity and fertility.

Geostatistical approaches integrated with multivariate analysis provide an effective framework to address this complexity, enabling the identification of spatial patterns of soil degradation and the selection of indicators that are highly sensitive to management-induced changes (13, 14). Previous studies indicate that PCA-based soil quality indices (SQIs) effectively discriminate different levels of soil quality under contrasting management practices, and that their integration with GIS allows for accurate and efficient spatial assessment of soil quality (15). In saline soils, electrical conductivity, sodicity-related variables, and nutrient availability consistently emerge as the main factors explaining variability in soil quality (16).

Recent applications in arid regions confirm the potential of SQIs to assess soil degradation and recovery processes. In northwestern China, long-term studies have shown that drip irrigation combined with mulching improves soil quality by 28–74%, although more than a decade is required for significant changes to stabilize (17). Likewise (18), demonstrated that the implementation of an SQI under irrigated conditions enabled the identification of salinity-sensitive indicators and the determination of thresholds beyond which accelerated soil degradation begins. In India (19), showed that salinity and sodicity—reflected by electrical conductivity (EC) and exchangeable sodium—constitute the main factors structuring SQIs in irrigated systems. Similarly, in the Songnen Plain (20), reported that EC, total salt content, and the sodium adsorption ratio (SAR) explain most of the edaphic variability in saline–sodic soils, confirming salinity as the dominant component driving soil degradation processes.

However, most of these studies were conducted in settings where salinization is gradual and secondary, rather than in soils that are inherently saline and subjected to heterogeneous management practices prior to the implementation of irrigation. Moreover, comparisons between irrigation systems regarding their effects on soil quality indicators remain poorly documented in arid agroecosystems of South America.

Consequently, the Santa Rita de Siguas irrigation scheme, in southern Peru, serves as a representative case, in which the incorporation of arid desert lands into agriculture has progressively increased since the arrival of irrigation water in 1934. One of the earliest studies conducted in 1974 reported 1,492 ha of agricultural land, of which 84% exhibited electrical conductivity values below 4 dS m^{-1} while 16% showed values between 10 and 30 dS m^{-1} (21). Currently, the irrigated area covers approximately 3,200 ha (22), implying the progressive incorporation of new desert lands into agricultural production. This expansion has occurred under uneven adoption of management practices, such as irrigation system, subsoiling, tillage methods, salt leaching, organic matter incorporation, irrigation frequency, and established crops selection. As a result, the irrigation scheme has likely evolved into an edaphic mosaic characterized by contrasts in physicochemical soil properties.

In this context, the objective of this study was to develop a spatially explicit weighted soil quality index (SQIw) and to evaluate the effects of contrasting irrigation systems (drip and surface) on soil salinity and fertility within an emerging irrigation scheme in the Peruvian coastal desert.

2 Materials and methods

2.1 Study area

The study was conducted in agricultural areas within the Santa Rita de Siguas irrigation scheme, located in the district of Santa Rita de Siguas, province and department of Arequipa, southern Peru. The irrigation scheme extends between latitudes 16°27′41.8″S – 16° 33′53.1″S, and longitudes 72°03′57.6″W and 72°10′17.9″W, at a mean elevation of 1,275 m above sea level (Figure 1). By 1974, the irrigated area covered approximately 1,492 ha (21) whereas it currently encompasses a total agricultural area of 3,235 ha (22). Soil sampling sites were selected within this area. The irrigation scheme is located on a high alluvial plain adjacent to the Siguas River valley, characterized by flat to gently sloping relief (1–2%) and soils developed on moderately coarse- to coarse-textured alluvial deposits (21). The study area exhibits arid climatic conditions, with a mean annual precipitation of 0.11 mm, calculated based on historical records from (23).

This scheme supports a diversified agricultural production system. At the sampling time, prickly pear (*Opuntia ficus-indica*), cultivated primarily for cochineal (*Dactylopius coccus*) production, was the dominant crop, accounting for approximately 40% of the sampled sites; other crops included forage maize, alfalfa, quinoa, onion, potato, garlic, and paprika pepper. Two irrigation systems coexist within the scheme: drip irrigation, predominantly used for prickly pear and vegetable crops, and surface irrigation, which comprises furrow irrigation for row crops and flood or border irrigation for alfalfa. Surface irrigation does not represent a homogeneous practice, varying according to crop type and rotation stage, as alfalfa is introduced as part of short-term rotations of approximately 1–2 years following annual crops. Although detailed irrigation management information (e.g., irrigation frequency, applied water depth, drainage conditions, and leaching fraction) was not systematically recorded during sampling, this characterization reflects the dominant irrigation practices under local farming conditions.

2.2 Soil sampling and laboratory analysis

A total of 930 composite soil samples were collected between June and December 2024 from 1-ha parcels randomly distributed across the study area to capture spatial heterogeneity (Figure 1). Parcel selection was based on voluntary farmer participation and field access authorization. Within each parcel, a systematic zig-zag pattern was employed to account for within-field variability (24). Soil samples were collected at 0–20 cm depth using a spade. Ten subsamples per site, within the recommended range of 4–16 subsamples (25), were collected and thoroughly homogenized in clean, non-galvanized containers. From the homogenized mixture, a composite sample of approximately 1.0 kg was taken. Samples were double-bagged in plastic, labeled with unique identifiers, and georeferenced using a handheld GPS. Although designated for 1-ha composite samples, the irregular parcel geometry resulted in a non-regular sampling grid with a minimum distance of 40 m between adjacent points.

Samples were analyzed at the Soil, Water and Foliar Laboratory Network of the National Institute of Agrarian Innovation (LABSAF-INIA). Analytical protocols were standardized for high sample throughput, focusing on essential fertility indicators rather than exhaustive geochemical speciation. Prior to physicochemical analysis, samples were air-dried (< 40 °C) and sieved to obtain a< 2 mm fraction according to the International Organization for Standardization (26). The variables analyzed included the following parameters and reference methodologies: sand, silt and clay content by the Bouyoucos hydrometer method (27); pH measured in a 1:1 soil-water suspension according to the United States Environmental

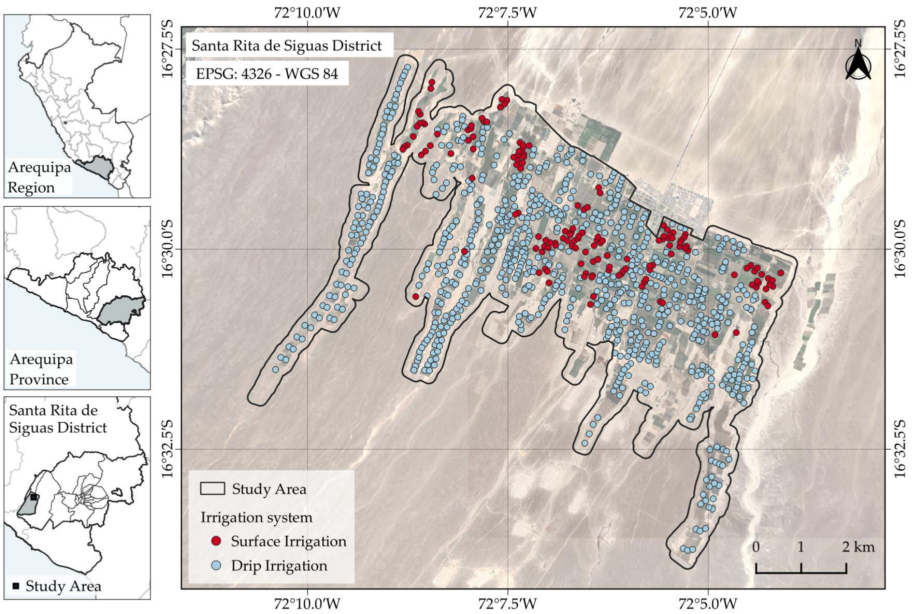

FIGURE 1
Location of soil sampling sites within the Santa Rita de Siguas irrigation scheme. Inset maps indicate administrative boundaries at regional, provincial, and district levels for geographic reference only.

Protection Agency method (28); electrical conductivity in a 1:5 soil-water extract (EC1:5) (29); organic matter (OM) by the Walkley–Black oxidation method; available phosphorus (Pav) by the Olsen method; available potassium (Kav) by 1N ammonium acetate extraction; and calcium carbonate (CCE) via acid neutralization (27). Although ECe is the standard for salinity assessment, EC1:5 was measured given its suitability for large-scale laboratory operations; the conversion procedure to ECe values is addressed in the (Supplementary Method S1).

2.3 Soil quality index development

The development of the weighted soil quality index (SQIw) followed a three-stage methodological framework: (1) screening soil indicators to establish a minimum data set (MDS); (2) transforming indicators into dimensionless scores; and (3) integrating scores into the weighted index.

2.3.1 Minimum data set selection

To minimize data redundancy and identify the most representative indicators, a screening process was applied to the total data set (TDS). Spearman's rank correlation coefficients were computed to assess the degree of association among all variable pairs and detect potential multicollinearity. Significant correlations ($p < 0.01$) were visualized using correlation matrix heatmaps to identify redundant variable groups. Indicator pairs exhibiting strong redundancy were defined as those with absolute correlation coefficients greater than 0.70 ($|\rho| > 0.70$). For each group of redundant variables, a single representative was selected based on its agronomic significance for soil quality assessment in arid agroecosystems. Redundant variables were subsequently excluded.

Complementary to this redundancy screening, a principal component analysis (PCA) was performed on the standardized TDS to quantify the explanatory power of the remaining candidates. Prior to analysis, variables with skewed distributions were log-transformed. The selection of the final MDS indicators was governed by a multi-criteria approach: (i) retention of principal components (PCs) with eigenvalues ≥ 1 (Kaiser criterion), while aiming to explain at least 60% of cumulative variance; (ii) selection of variables with high factor loadings (absolute value ≥ 0.60) within each retained PC; and (iii) exclusion of variables with low aggregate communality (< 0.60) in the global model, as they indicate a weak representation of the dataset's total variance.

Following the definition of the MDS indicators, a second specific PCA was executed exclusively on this subset to determine the final weighting factors W_i. This re-analysis ensures that the weights accurately reflect the relative contribution of each selected indicator's communality within the reduced index, calculated according to (Equation 1):

$$W_i = \frac{C_i}{\sum C} \tag{1}$$

where C_i is the variable's communality in the specific MDS-PCA, and $\sum C$ is the sum of communalities of all indicators included in the MDS.

2.3.2 Indicator scoring functions

Selected MDS indicators were transformed into dimensionless scores ranging from 0.1 to 1.0 to compare soil variables measured in different units. This scaling range allows limiting factors to significantly penalize the final score without assigning a zero value, thereby acknowledging that even degraded soils retain a baseline functional capacity.

Critical thresholds (x_1 and x_2) were defined using a hybrid approach, integrating agronomic criteria with the data distribution of soil properties observed in the study area. Thresholds for pH and sand content were aligned with USDA guidelines (30). Specifically, optimal ranges were defined for neutral pH (6.6–7.3) and loamy textures (< 50% sand), whereas severe limitations were assigned to strongly acidic/alkaline conditions and sandy classes (> 85%) due to chemical constraints and low water-holding capacity. Conversely, thresholds for salinity and fertility indicators were anchored to the dataset's statistical distribution to reflect local pedoclimatic variability. For electrical conductivity (EC1:5), the upper threshold (x_2) was set at 1.0 dS m^{-1}, corresponding to approximately the 20th percentile of the observed distribution. Using the texture-based conversion factor (CF = 10.2 ± 1.2; R^2 = 0.83) derived from (31), this threshold corresponds to an equivalent ECe of ~10.2 dS m^{-1}, which exceeds the tolerance threshold of the most salinity-sensitive crops present in the scheme. A sensitivity analysis of the EC1:5-to-ECe conversion and its propagated uncertainty is provided in Supplementary Figure 1 and Supplementary Table 2. Organic matter thresholds were anchored to the minimum observed value to normalize scores against the inherent scarcity of carbon in arid soils. For Kav, a full-range relative scoring was applied, following (32), with thresholds aligned to the minimum and maximum values to maximize discrimination between nutrient-depleted and enriched soils.

After establishing thresholds, indicators were standardized using linear scoring methods to assign a score to each variable, following the principles described by (33). The indicators were transformed according to their functional influence on soil quality. The "More is Better" (MB) function (Equation 2) was applied to OM and Kav as their availability correlate positively with soil fertility and nutrient status. The "Less is Better" (LB) function (Equation 3) was adopted for EC1:5 and sand content as excessive values negatively impact soil quality. For pH, which exhibits a unimodal (optimal range) response, the "Optimal Range" (OR) function (Equation 4) was developed to penalize deviations from the ideal range in both directions. The specific scoring functions and threshold values assigned to each indicator are summarized in Table 1.

$$M(x) = \begin{cases} 0.1, & x \le x_1 \\ 0.1 + 0.9\left(\frac{x - x_1}{x_2 - x_1}\right), & x_1 < x < x_2 \\ 1, & x \ge x_2 \end{cases} \tag{2}$$

$$L(x) = \begin{cases} 1, & x \le x_1 \\ 1 - 0.9\left(\frac{x - x_1}{x_2 - x_1}\right), & x_1 < x < x_2 \\ 0.1, & x \ge x_2 \end{cases} \tag{3}$$

TABLE 1 Scoring functions and threshold values for soil quality indicators.

Indicator	Unit	Function	Lower threshold (x_1)	Upper threshold (x_2)	Optimal ranges
pH	–	OR	5.5	8.4	6.6 - 7.3
EC1:5	dS m^{-1}	LB	0.0	1.0	–
OM	%	MB	0.5	2.0	–
Kav	mg kg^{-1}	MB	57.0	700.0	–
Sand	%	LB	50.0	85.0	–

OP, optimal range; LB, the lower, the better; MB, the more, the better.

$$O(x) = \begin{cases} 0.1 + 0.9(\frac{x-x_1}{L-x_1}), & x_1 \le x < L \\ 1, & L \le x \le U \\ 0.1 + 0.9(\frac{x_2-x}{x_2-U}), & U < x \le x_2 \end{cases} \quad (4)$$

Where x is the measured value; x_1 and x_2 denote the lower and upper thresholds, respectively; and L and U represent the lower and upper bounds of the optimal range.

2.3.3 Weight assignment and SQIw calculation

The SQIw was computed using the weighted additive approach (Equation 5):

$$SQI_w = \sum_{i=1}^{n} W_i N_i \quad (5)$$

where n is the total number of variables, W_i is the assigned weight, and N_i is the normalized indicator score. The resulting index was classified into five quality grades using equal intervals of 0.2, based on the index ranges utilized by (34). SQIw values were classified as follows: < 0.20 as "Very Poor"; 0.20–0.40 as "Poor"; 0.40–0.60 as "Acceptable"; 0.60–0.80 as "Good"; and ≥ 0.80 as "Optimal".

The weighted additive approach assumes compensatory relationships among indicators, where high scores in one variable can offset low scores in another. However, this assumption may lead to agronomically unrealistic classifications when critical constraints (such as extreme salinity) are partially masked by favorable values of other indicators. To address this limitation, a penalty factor of 0.7 was applied to samples exhibiting any indicator score ≤ 0.1, ensuring that soils with severe limitations are appropriately downgraded regardless of their performance in other attributes.

2.4 Geostatistical analysis

2.4.1 Spatial autocorrelation

Prior to spatial interpolation, an exploratory spatial data analysis (ESDA) was conducted to characterize the spatial structure of soil properties and guide the selection of the most appropriate interpolation method. The global spatial autocorrelation was evaluated for the SQIw and all selected soil indicators using Moran's I index (Equation 6) to test the null hypothesis of spatial randomness (35, 36). This index quantifies the degree to which similar values cluster spatially. An inverse distance spatial weight matrix based on the eight nearest neighbors (k = 8) was employed. Statistical significance was evaluated at $\alpha = 0.05$.

$$Moran's\ I = \frac{n}{\sum_{i=1}^{n}\sum_{j=1}^{n} w_{ij}} \cdot \frac{\sum_{i=1}^{n}\sum_{j=1}^{n} w_{ij}(y_i - \bar{y})(y_j - \bar{y})}{\sum_{i=1}^{n}(y_i - \bar{y})^2} \quad (6)$$

where n is the number of observations, w_{ij} is the spatial weight representing the degree of connection between neighboring samples i and j, y_i is the sampled value at location i, and $\bar{y}$ is the arithmetic mean of all sampled values. Moran's I values range from -1 to +1, where positive values indicate spatial clustering of similar values, values near zero suggest random spatial distribution, and negative values indicate spatial dispersion.

2.4.2 Semivariogram modeling and ordinary kriging

Experimental semivariograms $\gamma(h)$ were computed to quantify the spatial dependence structure of each soil variable according to (Equation 7):

$$\gamma(h) = \frac{1}{2N(h)} \sum_{i=1}^{N(h)} [Z(x_i) - Z(x_i + h)]^2 \quad (7)$$

where $N(h)$ is the number of data pairs separated by a lag distance h, and $Z(x_i)$ is the measured value at location x_i.

Prior to semivariogram analysis, variables exhibiting skewed distributions (EC15, OM, and Pav) were log-transformed to stabilize variance. Experimental semivariograms were computed using a lag distance (width) of 50 m, consistent with the minimum inter-point distance of the sampling grid (~40 m), and a maximum cutoff distance of 3500 m. Theoretical models (Spherical, Exponential, or Gaussian) were fitted to the experimental semivariograms based on the minimization of the Sum of Squared Errors (SSE). The degree of spatial dependence was classified using the nugget-to-sill ratio ($C_0/(C_0 + C)$) following (37): strong (< 0.25), moderate (0.25–0.75), and weak (> 0.75).

Ordinary Kriging (OK) was employed for spatial interpolation onto a 10 m resolution grid. This pixel size was selected for cartographic presentation purposes, to produce visually continuous interpolated surfaces, and does not imply that the spatial model resolves variability at that scale. The effective spatial resolution of the predictions is governed by the semivariogram parameters described above.

For log-transformed variables, predictions were back-transformed to the original scale using a bias-corrected lognormal back-transformation to avoid the underestimation associated with simple exponentiation (38). The SQIw was calculated using the interpolated raster layers of the MDS indicators. Cartographic representation and map production were performed in QGIS v.3.40.6 (39).

2.4.3 Cross-validation

To objectively assess interpolation performance, Ordinary Kriging (OK) was evaluated using 10-fold cross-validation. The dataset was randomly partitioned into 10 subsets; in each iteration, one subset was reserved for validation while the remaining nine were used for spatial prediction using the previously fitted variogram model.

Predictive accuracy was quantified using four statistical metrics: root mean square error (RMSE, Equation 8), mean absolute error (MAE, Equation 9), mean error (ME, Equation 10), and coefficient of determination (R^2, Equation 11), calculated as:

$$RMSE = \sqrt{\frac{1}{n}\sum_{i=1}^{n}(y_i - \hat{y}_i)^2} \quad (8)$$

$$MAE = \frac{1}{n}\sum_{i=1}^{n}|y_i - \hat{y}_i| \quad (9)$$

$$ME = \frac{1}{n}\sum_{i=1}^{n}(y_i - \hat{y}_i) \quad (10)$$

$$R^2 = 1 - \frac{\sum_{I=1}^{n}(y_i - \hat{y}_i)^2}{\sum_{I=1}^{n}(y_i - \bar{y})^2} \quad (11)$$

where n is the number of observations, y_i is the observed (measured) value at location i, $\hat{y}_i$ is the predicted value at location i obtained through cross-validation, and $\bar{y}$ is the mean of all observed values.

Optimal predictive performance is indicated by minimized RMSE and MAE, and an ME value near zero indicating unbiased predictions. The R^2 is reported as a complementary descriptor of the observed-predicted association; however, due to the inherent smoothing effect of Ordinary Kriging, predicted values tend to regress toward the mean, which may constrain the observed-predicted variance and yield R^2 values that may not fully reflect the predictive capacity of the interpolation. All validation metrics were computed in original measurement units; for log-transformed variables (EC1:5 and OM), cross-validation predictions were back-transformed using bias-corrected lognormal back-transformation prior to metric calculation.

2.5 Effect of irrigation system

As described in Section 2.1, two irrigation systems were identified within the scheme: drip irrigation (n = 782) and surface irrigation (n = 148), representing 84.1% and 15.9% of the sampled parcels, respectively. Based on the 1-ha composite parcel design, these figures correspond to an estimated coverage of approximately 782 ha and 148 ha for drip and surface irrigation, respectively, though they should be interpreted as approximations given the non-stratified nature of the sampling design.

To evaluate the influence of irrigation system on soil chemical properties (EC1:5, Pav, and Kav), the Mann-Whitney U test was employed. This non-parametric approach was selected due to the non-normal distribution of the data (Kolmogorov-Smirnov, $p < 0.05$). To account for the group imbalance and provide a standardized magnitude of differences independent of sample size, the rank-biserial correlation (r_{rb}) was calculated as the effect size (40). Following (41), r_{rb} values were interpreted as negligible (< 0.10), small (0.10–0.30), medium (0.30–0.50), or large (≥ 0.50). Differences were visualized using combined violin and boxplots to facilitate the interpretation of variability and central tendency between irrigation systems.

2.6 Statistical analysis

All statistical analyses were performed using R software v.4.4.2 (42). Prior to multivariate and geostatistical analyses, distributional properties of soil variables were evaluated using the Kolmogorov-Smirnov test. Variables exhibiting pronounced positive skewness were natural log-transformed to approximate normality and stabilize variance. Log-transformed values were used for Principal Component Analysis (after z-score standardization), spatial autocorrelation analysis, and Ordinary Kriging. Geostatistical predictions were back-transformed using the bias-corrected exponential approach to express results in original units. Conversely, descriptive statistics, Spearman correlations, and the Mann-Whitney U test were conducted on untransformed data, consistent with the rank-based nature of these non-parametric methods.

Descriptive statistics were calculated using the base R functions. Spearman rank correlations were computed using the *psych* package (43) and visualized with *corrplot* (44). Principal Component Analysis was implemented with *FactoMineR* (45). Spatial autocorrelation (Moran's I) was assessed using the *spdep* package (46), while geostatistical modeling and kriging were performed with *gstat* (47). The effect size for the Mann-Whitney U test was calculated using the *effectsize* package (48), and statistical visualizations were generated using *ggstatsplot* (49).

3 Results

3.1 Descriptive statistics

Descriptive analysis (Table 2) characterized the soil conditions of the study area as predominantly sandy (mean > 70%) with an alkaline reaction (mean pH of 7.49). These properties exhibited the lowest spatial variability within the dataset (CV< 16%). In contrast, Pav, EC1:5, and exNa showed severe heterogeneity (CV > 90%) and pronounced positive skewness (> 3.0), associated with the presence of localized accumulation "hotspots" rather than a uniform distribution across the irrigation scheme. OM and CCE exhibited moderate variability (CV ranging from 48 to 57%), while mean values reflected the low carbon contents typical of arid agroecosystems. Finally, the Kolmogorov–Smirnov test confirmed that none of the variables followed a normal distribution ($p < 0.05$). This pervasive lack of normality, driven by the pronounced skewness of the chemical data, justifies the use of non-parametric methods for assessing associations among variables.

TABLE 2 Descriptive statistics and normality test results of variables in the study area (n = 930).

Variable (unit)	Mean ± SD	Median (Q_1 − Q_3)	Range (min − max)	CV (%)	skewness	K-S test (*p*-value)
pH (1:1)	7.49 ± 0.35	7.50 (7.30 – 7.70)	4.80 – 8.60	4.71	−0.97	< 0.001
EC1:5 (dS m^{-1})	2.37 ± 2.18	2.17 (0.85 – 3.08)	0.02 – 23.70	91.86	3.27	< 0.001
OM (%)	1.19 ± 0.67	1.10 (0.70 – 1.50)	0.30 – 8.50	56.64	2.66	< 0.001
Pav (mg kg^{-1})	48.59 ± 73.36	32.90 (17.45 – 59.98)	1.30 – 990.10	150.97	7.02	< 0.001
Kav (mg kg^{-1})	538.12 ± 253.98	513.89 (361.83 – 701.30)	57.20 – 1663.70	47.20	0.63	0.017
Sand (%)	70.15 ± 11.18	72.00 (67.00 – 76.00)	7.00 – 92.00	15.94	−2.37	< 0.001
Silt (%)	18.93 ± 9.18	18.00 (13.00 – 22.00)	0.00 – 66.00	48.49	1.85	< 0.001
Clay (%)	10.89 ± 3.77	10.00 (8.00 – 13.00)	4.00 – 28.00	34.66	1.23	< 0.001
CCE (%)	2.27 ± 1.09	2.10 (1.50 – 3.00)	0.00 – 7.50	47.97	0.77	< 0.001
exNa (cmol kg^{-1})	4.07 ± 3.96	2.89 (1.94 – 4.53)	0.54 – 47.17	97.21	4.20	< 0.001

SD, Standard Deviation; Q1, 25th percentile; Q3, 75th percentile; CV, Coefficient of Variation; K-S, Kolmogorov-Smirnov test. EC1:5, Electrical conductivity of the 1:5 soil-to-water extract; OM, Organic Matter; Pav, available phosphorus; Kav: available potassium; CCE, calcium carbonate equivalent; exNa, exchangeable sodium.

3.2 Correlation analysis

To mitigate the influence of non-normal data distribution and to detect multicollinearity among soil properties, Spearman's rank correlation coefficients (ρ) were calculated (Figure 2). This analysis served as a preliminary screening step to identify redundant variables that could be excluded from the Minimum Data Set (MDS).

The most prominent structural relationship was observed within the physical fraction, where sand content exhibited a very strong negative correlation with silt (ρ = −0.89, p< 0.001) and a weak-to-moderate negative correlation with clay (ρ = −0.37, p< 0.01). To avoid redundancy in further analysis, silt was excluded due to its high collinearity, retaining only sand and clay from the physical fraction.

Within the group of chemical variables, EC1:5 exhibited the highest positive correlations with both Kav and exNa (ρ = 0.62, p< 0.001). Furthermore, exNa also exhibited negative correlation with the sand fraction and positive correlations with silt and CCE, the strongest of which was with silt (ρ = 0.21, p< 0.001).

Conversely, fertility indicators such as OM and pH displayed generally weak correlations with other soil properties ($|\rho|$< 0.30). Although CCE showed a moderate inverse association with sand content (ρ = −0.37), it was excluded from the final MDS in order to prioritize pH and EC1:5 as the main chemical constraints.

3.3 PCA and MDS selection

Principal Component Analysis (PCA) was performed on the Total Data Set (TDS) to identify the most representative indicators and reduce data dimensionality. Prior to analysis, variables exhibiting skewness greater than 3 (EC1:5, OM, Pav, and exNa) were log-transformed to approximate normality and minimize the influence of outliers. Initial assessment revealed that most variables exhibited high communalities (> 0.60); however, Pav and exNa showed the lowest explained variance (0.543 and 0.583, respectively) within the global model (Table 3), and were therefore excluded as they did not meet the minimum communality threshold. Among textural fractions, silt was excluded on the basis of its comparatively lower communality (0.614) within the global PCA model, the lowest among the remaining variables, despite marginally exceeding the 0.60 threshold.

The final Minimum Data Set (MDS) comprised five indicators: pH, EC1:5, OM, Kav, and sand. A subsequent PCA performed exclusively on the MDS retained three principal components explaining 76.8% of the cumulative variance (Table 4). PC1 (32.1% of variance) was dominated by EC1:5 and Kav, representing the salinity-fertility gradient. PC2 (23.5%) captured the pH-OM relationship, reflecting the organic matter-alkalinity interaction characteristic of arid soils. PC3 (21.2%) was primarily loaded by sand content, representing the textural constraint on water and nutrient retention. All five MDS variables were associated with a dominant component within this structure, satisfying the indicator representation criterion established in the methods (|loading| > 0.60).

Final weighting factors derived from the MDS-specific PCA assigned the highest influence to Sand (0.223) and EC1:5 (0.211), followed by Kav (0.206), OM (0.181), and pH (0.180) (Table 3). This weighting structure reflects the dominant role of textural and salinity constraints in determining soil quality within the irrigation scheme.

3.4 Soil quality index

Based on the PCA weights, the specific Weighted Additive Index (SQIw) was calculated for each of the 930 sampling locations across the Santa Rita de Siguas irrigation scheme, as presented in Equation 12:

$$SQI_w = 0.223 \cdot S_{Sand} + 0.211 \cdot S_{EC} + 0.206 \cdot S_{Kav} + 0.181 \cdot S_{OM} + 0.180 \cdot S_{pH} \quad (12)$$

where S_i is the scoring function value for each MDS indicator (0.1–1).

The integration of PCA-derived weights with the penalty factor revealed a predominantly degraded state across the sampling locations. The resulting SQIw distribution shows that the mean (0.408 ± 0.115) marginally falls within the "Acceptable" category while the median (0.380) remains within "Poor", indicating that the central tendency is concentrated near the class boundary. Moderate spatial variability was observed (CV = 28.2%), and the high frequency of penalized sampling points, which exceeding three-quarters of the total, suggests that severe salinity limitations are a

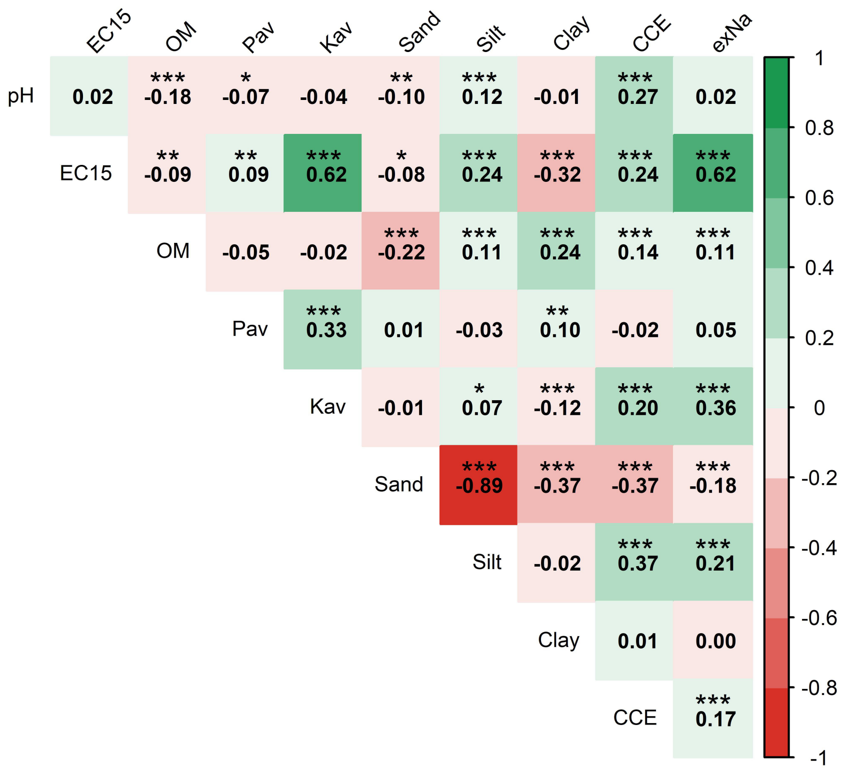

FIGURE 2
Spearman's correlation matrix of the total data set (TDS) components for soil quality index assessment. The color gradient indicates the strength and direction of the correlation: green for positive and red for negative. Statistical significance is denoted by asterisks: *$p < 0.05$, **$p < 0.01$ and ***$p < 0.001$. Values without an asterisk are not statistically significant.

systematic rather than localized feature of the irrigation scheme (Table 5).

This widespread degradation is characterized by moderate spatial variability (CV = 28.2%). The penalization mechanism played a decisive role in these results. The fact that over three-quarters of the individual sampling points triggered this penalty indicates that severe limitations are not isolated incidents but a systemic feature of the study area.

TABLE 3 PCA-based communality and weighting of TDS and MDS.

Variable	TDS		MDS	
	COM	Weight	COM	Weight
pH (1:1)	0.626	0.088	0.692	0.180
EC1:5 (dS m^{-1})	0.792	0.112	0.805	0.211
OM (%)	0.874	0.124	0.694	0.181
Pav (mg kg^{-1})	0.543	0.077	–	–
Kav (mg kg^{-1})	0.674	0.095	0.792	0.206
Sand (%)	0.954	0.135	0.854	0.223
Silt (%)	0.816	0.115	–	–
Clay (%)	0.614	0.087	–	–
CCE (%)	0.602	0.087	–	–
exNa (cmol kg^{-1})	0.583	0.082		

COM, communality; TDS, total data set; and MDS, minimum data set.

At the individual sampling sites, salinity (EC1:5) emerged as the primary factor driving soil degradation, acting as the dominant constraint in the vast majority of cases. The low frequency of "Good" and "Optimal" classifications, which together account for less than 9% of the total samples, further highlights the limited agronomic potential currently available in the study area. These localized results provide the essential statistical context for the spatial patterns examined in the following section.

3.5 Spatial analysis

3.5.1 Spatial autocorrelation

Exploratory spatial data analysis (ESDA) was conducted to characterize the spatial structure of soil properties prior to interpolation. Global Moran's I statistics were calculated using a k-nearest neighbors spatial weight matrix ($k = 8$) with row standardization (Table 6).

Global spatial analysis confirmed that all MDS indicators and the SQIw exhibited significant clustered patterns ($p < 0.001$, Z-scores ranging from 17.77 to 25.52), rejecting the hypothesis of spatial randomness. Sand content displayed the highest clustering index (I = 0.40), reflecting the geological continuity of alluvial deposits. Similarly, EC1:5 and Kav showed comparable moderate autocorrelation (I ≈ 0.39), suggesting that salinity and potassium distributions are driven by common management-induced processes. In contrast, pH and the SQIw exhibited weaker clustering (I = 0.28), indicating higher randomness at the sampling scale.

TABLE 4 PCA output for the MDS including eigenvalues, percentage of variance explained, and factor loadings of component matrix variables.

PCs	PC1	PC2	PC3	PC4	PC5
Eigenvalue	1.606	1.175	1.058	0.777	0.385
Variance (%)	32.121	23.493	21.155	15.537	7.694
Cumulative Variance (%)	32.121	55.614	76.769	92.306	100.000
Factor loadings for each variable					
pH	0.009	**−0.764**	−0.329	0.552	0.058
EC1:5 (dS m^{-1})	**0.897**	0.027	−0.001	−0.075	0.435
OM (%)	−0.096	**0.765**	−0.315	0.548	0.079
Kav (mg kg^{-1})	**0.887**	0.062	0.051	0.163	−0.426
Sand (%)	−0.078	−0.015	**0.921**	0.375	0.072

Principal Components (PCs) with eigenvalues > 1.0 were retained. Bold values indicate the dominant indicators within each PC based on absolute factor loadings > 0.60.

While these structural patterns justify the application of geostatistical interpolation, the moderate magnitude of Moran's I values (< 0.50) highlights substantial short-range heterogeneity, which may constrain prediction accuracy.

3.5.2 Semivariogram modeling

The analysis of experimental semivariograms (Figure 3) indicated that only pH was best described by a Spherical model, whereas Exponential models were fitted to all other variables, including EC1:5, OM, Kav, Sand, and the final SQIw.

The fitted semivariogram parameters (Table 7) revealed distinct spatial dependence patterns: EC1:5 exhibited strong spatial dependence (nugget/sill< 0.25), suggesting that its spatial variability may be largely associated with spatially structured factors operating at fine scales. In contrast, pH, Kav, Sand, OM, and SQIw showed moderate spatial dependence (nugget/sill ratios ranging from 0.28 to 0.44), suggesting a possible combined influence of structured spatial variance and random local variability.

Effective ranges varied widely, reflecting different processes governing spatial distribution. Short ranges for SQIw (260 m) point to localized anthropogenic effects such as irrigation management. In contrast, Sand (1,720 m) and OM (350 m) displayed broader spatial continuity linked to pedogenic or geological factors.

3.5.3 Cross-validation performance

Ten-fold cross-validation was performed to evaluate the predictive accuracy of Ordinary Kriging (OK) interpolation (Table 8). Validation metrics were computed in original measurement units to ensure practical interpretability. Results confirmed approximately unbiased predictions across all variables (ME ≈ 0). Predictive association, expressed as the coefficient of determination (R^2), reflected the moderate nugget effects observed in the semivariogram analysis, with Kav showing the strongest observed-predicted correspondence and SQIw the weakest (R^2 = 0.246, RMSE = 0.100), suggesting that short-range variability below the sampling spacing limits predictive performance at point locations. The near-zero ME values across all variables support the suitability of these models for delineating regional soil management zones.

3.5.4 Spatial distribution of soil properties and SQIw

Ordinary Kriging interpolation revealed distinct spatial patterns across the irrigation scheme (Figure 4). Variables with comparatively low spatial variability, namely pH and organic matter, showed largely homogeneous distributions. Soil pH was predominantly neutral to slightly alkaline, with 71.7% of the area in the 7.3–7.7 range and only 12.9% reaching moderately alkaline conditions (7.7–8.6). Organic matter content was consistently low across the scheme, with 85.7% of the area falling below 1.5%, and values exceeding 2.0% restricted to 2.99% of the total area, distributed along the western margins.

In contrast, soil salinity and sand content exhibited more pronounced spatial gradients. Soil salinity (EC1:5) showed a critical gradient concentrated in the central and northeastern sectors, where moderate-to-high salinity conditions (2.0–8.0 dS m^{-1}) covered 48.7% of the area, while low-salinity soils (< 2.0 dS m^{-1}) dominated the remaining 51%. Extreme salinity values (> 8.0 dS m^{-1}) were confined to a negligible fraction (0.23%). Sand content followed a similarly directional pattern, with coarse-textured soils (70–92%) covering 61.3% of the area and finer-textured materials (< 50%) restricted to 4.2%.

Available potassium showed an intermediate distribution, dominated by adequate levels in the 350–700 mg kg^{-1} range, which accounted for 70.5% of the area, followed by high values (700–900 mg kg^{-1}) covering 17.6%. Deficient concentrations (< 250 mg kg^{-1}) and very high values (> 900 mg kg^{-1}) were each restricted to less than 4% of the total area, forming spatially isolated hotspots.

The spatial distribution of SQIw across the irrigation scheme revealed a landscape dominated by intermediate quality classes (Figure 5). Soils classified as "Poor" (0.2–0.4) accounted for 46.7% of the interpolated area and were predominantly distributed in sectors associated with higher salinity, while "Acceptable" soils (0.4–0.6) covered 53.1% and formed spatially continuous transitional zones. A negligible fraction (< 1%) was classified as "Good", confined to a narrow elongated sector in the northwestern portion

TABLE 5 Summary statistics, quality classification, and limiting factors of the penalized soil quality index (SQIw) in Santa Rita de Siguas (n = 930).

SQIw statistics		Quality class	n (%)	Primary limiting factor	n (%)
Mean ± SD	0.408 ± 0.115	Very Poor	1 (0.1)	EC1:5	714 (76.8)
Median	0.380	Poor	537 (57.7)	OM	77 (8.3)
Range	0.178 – 0.810	Acceptable	309 (33.2)	Kav	71 (7.6)
CV (%)	28.2	Good	81 (8.7)	Sand	55 (5.9)
		Optimal	2 (0.2)	pH	13 (1.4)

10.3389/fsoil.2026.1789869

TABLE 6 Global Moran's I index for spatial autocorrelation of soil properties and soil quality index.

Variable	Transformation	Moran's I	Z-score	*p*-value	Spatial pattern
pH	None	0.28	18.20	< 0.001	Clustered
EC1:5	Log	0.39	24.89	< 0.001	Clustered
OM	Log	0.36	22.93	< 0.001	Clustered
Kav	None	0.39	24.89	< 0.001	Clustered
Sand	None	0.40	25.52	< 0.001	Clustered
SQIw	None	0.28	17.77	< 0.001	Clustered

of the study area. No areas reached "Very Poor" or "Optimal" conditions, indicating the absence of extreme soil quality states within the evaluated scheme. The areal distribution of all analyzed edaphic variables is summarized in Supplementary Table 1.

The areal class proportions derived from the interpolated surface differ from the sample-based statistics reported in Section 3.4, where the mean SQIw (0.408) marginally falls within the "Acceptable" category while the median (0.380) remains within "Poor", suggesting that the central tendency of the point distribution is concentrated near the class boundary. This discrepancy is consistent with the expected difference in spatial support between point-based sample statistics and kriged areal estimates, as the interpolated surface assigns equal spatial weight to all predicted locations regardless of sampling density.

3.6 Irrigation system effects

Mann-Whitney U tests revealed statistically significant differences between irrigation systems for all three evaluated chemical properties (Figure 6); however, the rank-biserial correlation indicated that the practical magnitude of these differences varied substantially across variables.

The most agronomically relevant contrasts were observed for EC1:5 and Kav, with drip-irrigated soils exhibiting median values approximately 318% (drip: 2.38, surface: 0.57 dS m^{-1}) and 100% (drip: 559.5, surface: 279.9 mg kg^{-1}) higher than surface-irrigated soils, respectively, both statistically significant ($p< 0.001$) and corresponding to large effect sizes (r_{rb} = 0.573 and 0.654, respectively). These results are consistent with the restricted wetting volume characteristic of drip systems, which promotes salt and nutrient accumulation in the rhizosphere in the absence of adequate leaching fractions. In contrast, although the difference in Pav was statistically significant (p = 0.018), the associated effect size was small (r_{rb} = 0.122), indicating limited practical relevance despite the large total sample size.

4 Discussions

4.1 Spatial variability and general characterization of the study area

Soil properties exhibited strong variability and non-normal distributions, which is typical of agricultural soils at a regional scale. This behavior reflects the combined influence of pedogenesis, management history, and spatial heterogeneity (37, 50).

Electrical conductivity (EC1:5), pH, carbonate content, and organic matter (OM) exhibited distinct spatial contrasts that are consistent with irrigated arid environments. Soil pH showed low spatial variability (CV ≈ 4.7%), which is consistent with the buffering effect of carbonates and the limited leaching of base cations under arid climatic conditions (51). In contrast, EC1:5 displayed very high variability (CV ≈ 92%), reflecting the heterogeneous accumulation and redistribution of salts controlled by irrigation water quality, leaching efficiency, and soil drainage conditions (52, 53). Soil organic matter and carbonates exhibited moderate to high variability (CV ≈ 48–57%), a pattern that is typical of arid soils subjected to contrasting management practices and varying degrees of organic residue and calcareous amendments (54, 55).

Available phosphorus and potassium (Pav and Kav) revealed the strongest spatial contrasts, reflecting the superposition of inherent edaphic conditions and a long history of heterogeneous agricultural management. The extreme variability of Pav is consistent with its low mobility and strong regulation by cumulative fertilizer applications and fixation processes in neutral to alkaline soils with carbonate presence. This leads to highly localized patterns of deficiency and accumulation (56–58). In contrast, although Kav largely reflects parent material inheritance typical of arid soils, its partial redistribution under irrigation and differential management, particularly in coarse-texture soils with low retention capacity, contributes to the development of spatial gradients that are highly relevant for site-specific nutrient management (59, 60).

Textural fractions showed moderate variability and strong interdependence. Because soil texture governs water retention, nutrient dynamics, and solute transport (51, 61), the inverse relationships among sand, silt, and clay suggest that their simultaneous inclusion in soil quality indices may be redundant. This supports the need for dimensionality reduction prior to SQI construction (62, 63).

4.2 Soil property correlations and their implications for soil quality index development

The Spearman correlation matrix (Figure 2) revealed statistically significant relationships ($p < 0.01$) among soil physicochemical properties, enabling the identification of redundant variables and

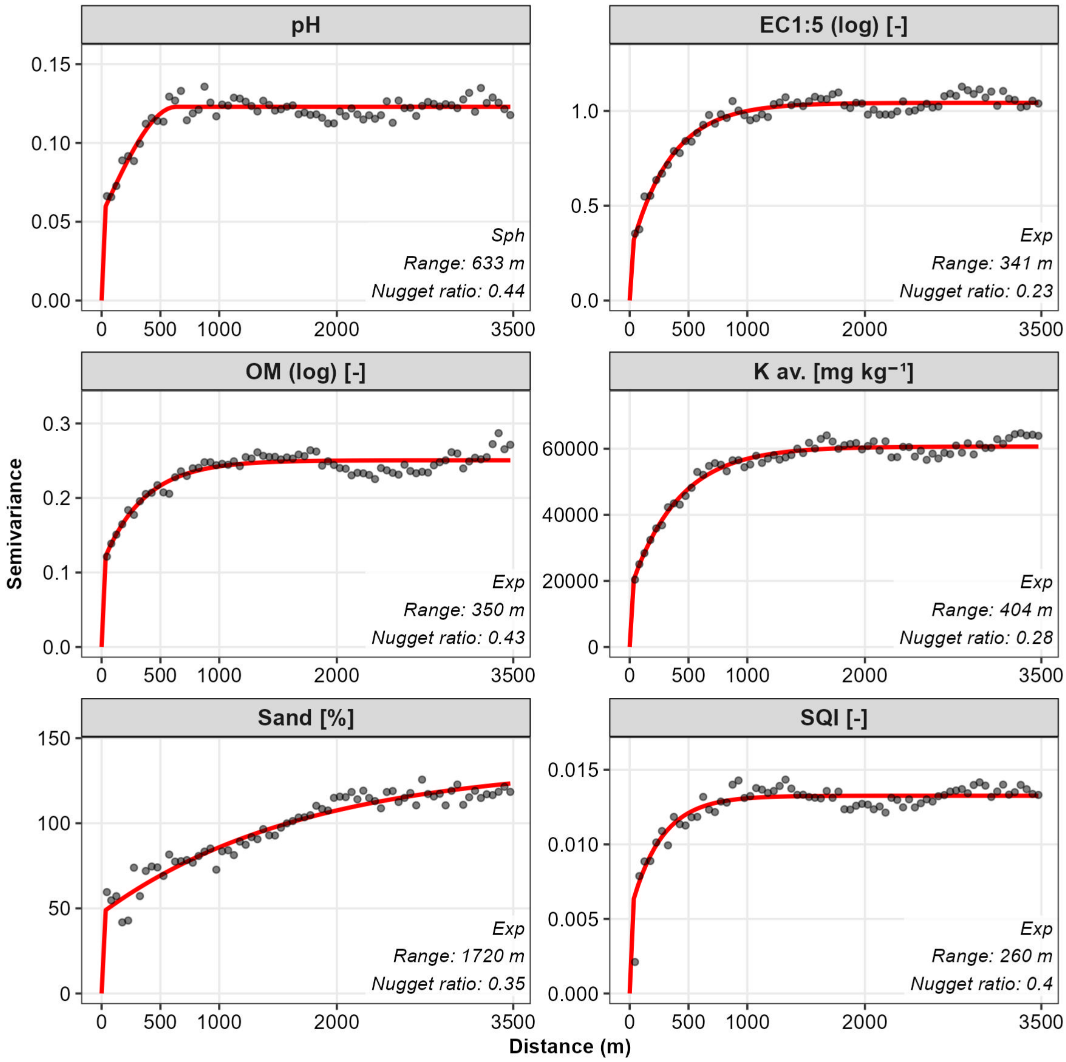

FIGURE 3
Experimental semivariograms and fitted theoretical models for selected soil quality indicators. Points represent the experimental semivariance values $\gamma(h)$, while solid lines depict the best-fitted theoretical models (exponential or spherical) used for ordinary kriging interpolation. Data for EC and OM are log-transformed.

the selection of representative indicators for the weighted soil quality index (SQIw) construction. Preliminary screening of indicators through correlation analysis ensures that the SQIw captures key soil processes without redundancy (1).

Correlations among textural fractions (sand, silt, and clay) reflect well-established pedological relationships associated with the control of water retention and nutrient dynamics (61). In particular, the strong negative correlations between sand and fine fractions confirm their

TABLE 7 Best-fitted semivariogram models and geostatistical parameters for soil properties and soil quality index (SQIw).

Variable	Transformation	Model	Nugget (C_0)	Structural (C)	Sill ($C_0 + C$)	Range (m)	SD ratio	Class
pH	None	Sph	0.054	0.069	0.123	633	0.44	Moderate
EC1:5	Log	Exp	0.242	0.801	1.043	341	0.23	Strong
OM	Log	Exp	0.109	0.142	0.251	350	0.43	Moderate
Kav	None	Exp	16796.674	43875.592	60672.266	404	0.28	Moderate
Sand	None	Exp	47.204	87.807	135.011	1720	0.35	Moderate
SQIw	None	Exp	0.005	0.008	0.013	260	0.4	Moderate

Variables with skewed distributions were log-transformed prior to geostatistical analysis. C_0, Nugget effect; C, Structural variance; Range, Effective range of spatial dependence; SD Ratio, Spatial Dependence Ratio ($C_0/(C_0 + C)$), classified as Strong (< 0.25), Moderate (0.25 - 0.75), or Weak (> 0.75) following (37). Exp, Exponential; Sph, Spherical.

TABLE 8 Cross-validation results of ordinary kriging interpolation for soil properties and soil quality index (SQIw).

Property	Transformation	RMSE	MAE	ME	R^2
pH	None	0.299	0.212	-0.001	0.282
EC15	Log	1.833	1.164	-0.272	0.290
OM	Log	0.547	0.374	-0.018	0.340
Kav	None	194.035	143.856	1.861	0.416
Sand	None	8.750	5.692	-0.053	0.387
SQIw	None	0.100	0.075	0.000	0.246

Validation statistics calculated on prediction data in original units (back-transformed for Log models). RMSE, Root Mean Square Error; MAE, Mean Absolute Error; ME, Mean Error (Bias); R^2, Coefficient of Determination. Transformation indicates the scale used for semivariogram modeling.

mutually exclusive nature and suggest partial redundancy, thereby justifying their screening during the selection of the minimum data set (MDS) for the SQIw construction (64).

Significant associations between EC1:5 and other chemical and textural properties indicate that salinity acts as an integrative indicator of edaphic processes related to salt accumulation and its interaction with the soil matrix (65). Owing to its high sensitivity to changes in soil chemical conditions, EC1:5 is considered a key variable in soil quality assessments (64). However, its simultaneous inclusion with strongly correlated variables should be carefully evaluated to avoid overrepresentation within the SQIw.

Positive correlations between nutrients such as Pav and Kav reflect soil accumulation processes and chemical availability. This is consistent with the behavior observed in inorganic phosphorus pools and plant phosphorus-use efficiency, as reported in soil quality studies (66). In this context, multivariate analysis enables the identification of the most representative soil variables, thereby avoiding the simultaneous inclusion of strongly correlated properties in the calculation of the soil quality index (15).

Soil organic matter reflects the integration of multiple soil functions, including fertility, structure, and buffering capacity,

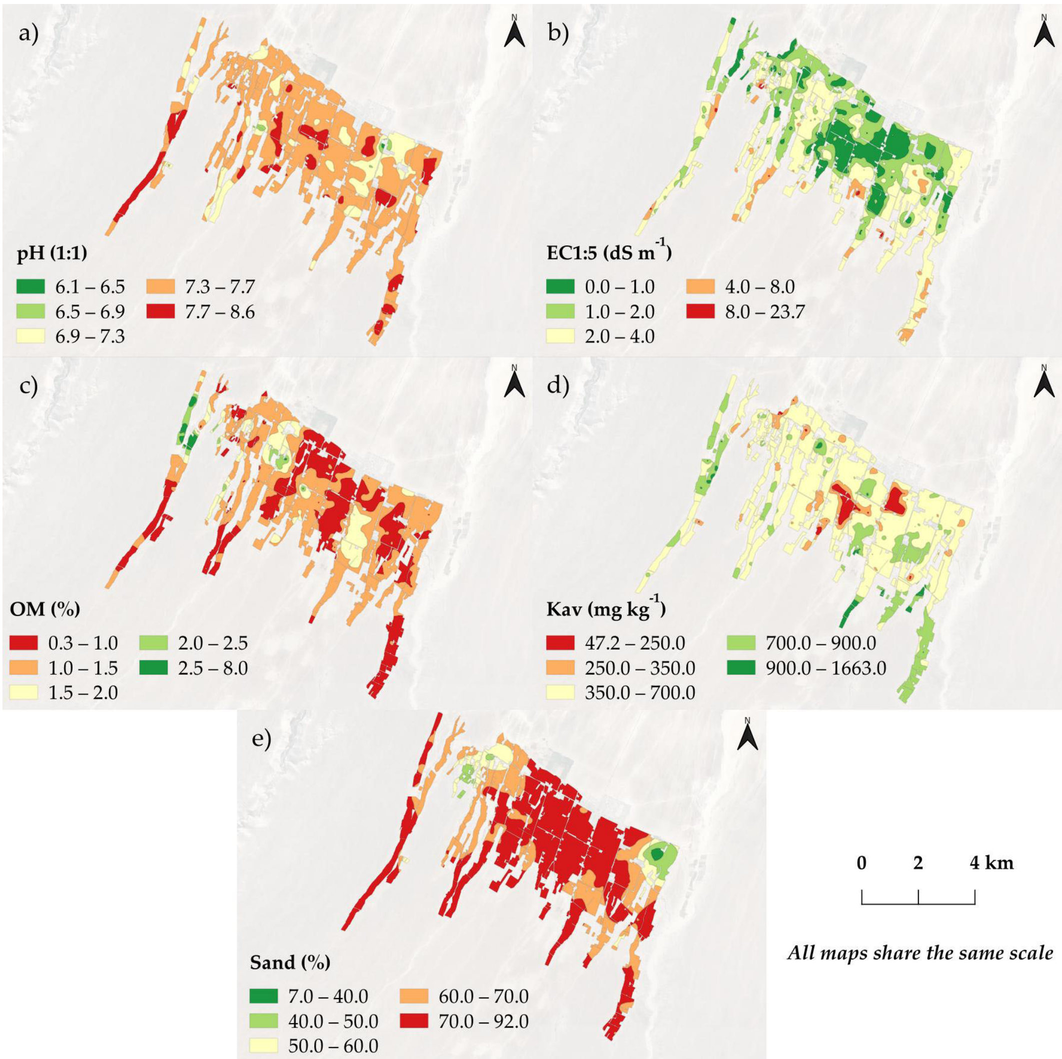

FIGURE 4
Spatial distribution of key soil indicators across the Santa Rita de Siguas irrigation scheme, derived from ordinary kriging (OK) interpolation. **(a)** pH, **(b)** electrical conductivity (EC1:5), **(c)** organic matter (OM), **(d)** available potassium (Kav), and **(e)** sand content. Classification thresholds are bounded by the minimum and maximum values observed in the field dataset. The predicted spatial range is narrower than the observed data range due to the smoothing effect inherent to OK interpolation.

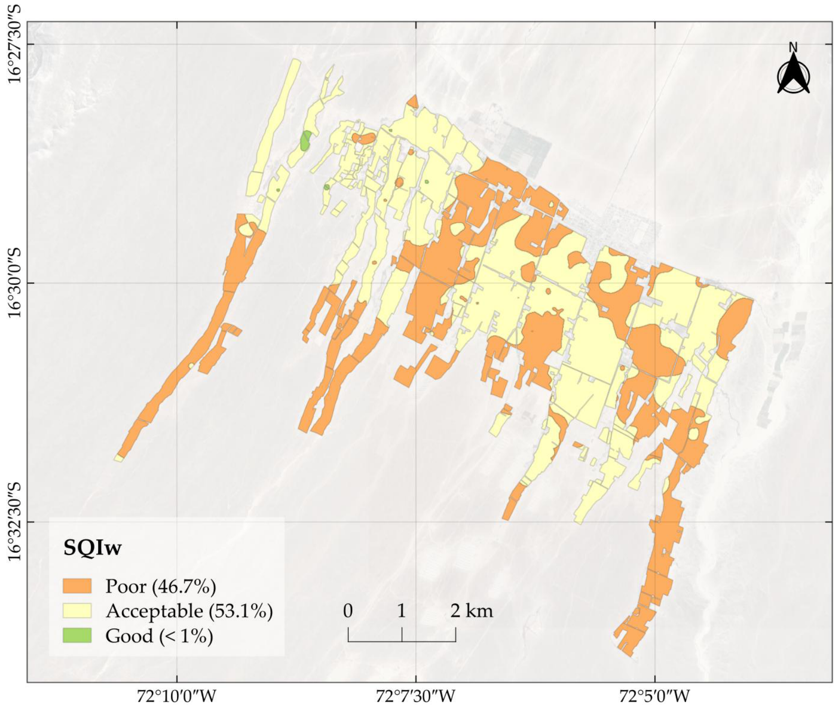

FIGURE 5
Spatial distribution map of the weighted soil quality index (SQIw) within the study area. Three classes were identified, with "Acceptable" and "Poor" dominating the study area and "Good" representing a negligible proportion.

and its assessment contributes to understanding soil quality as a dynamic and multifunctional system (67). Soil organic matter is an essential indicator of soil quality, as it integrates multiple functions and allows discrimination of the effects of different management systems, even when its correlations with other parameters vary (68, 69).

The Spearman correlation matrix was used as a preliminary step prior to multivariate analysis to reduce the dimensionality of the total data set (TDS) and to select a representative minimum data set (MDS) for soil quality assessment (70). This procedure enhances the interpretability of the soil quality index (SQI) and strengthens its scientific robustness.

The correlations shown in Figure 2 support the selection of chemical and physical, confirming the SQI as an integrative tool for evaluating soil quality in agricultural systems (71).

4.3 Soil quality index: development and interpretation

The weighted soil quality index (SQIw) was constructed based on a minimum set of indicators objectively selected through multivariate analyses, specifically Principal Component Analysis (PCA) to define the Minimum Data Set (MDS), using factor loadings to define the relative contribution of each variable. This approach is widely applied in soil quality studies because it reduces redundancy among correlated indicators and avoids subjective variable selection, ensuring that the index captures the main functional gradients of the edaphic system (67, 72). In this study, sand fraction, electrical conductivity (EC), available potassium (Kav), organic matter (OM), and pH emerged as the most representative indicators, integrating inherent soil properties and cumulative responses to agricultural management in irrigated arid environments (1).

The spatial distribution of the SQIw was exclusively concentrated within intermediate soil quality categories ("Poor" and "Acceptable"), with only a marginal occurrence of "Good" soils (< 1%) restricted to localized sectors. This pattern has been documented in agricultural systems established on naturally saline soils in arid regions, where long-term recovery gradually improves soil quality, yet SQI values remain within intermediate ranges (0.307–0.339) even after 20 years of agricultural management (73). The absence of optimal categories reflects these inherent structural limitations, whereas the lack of a "Very Poor" class indicates that the system retains basic functionality without critical degradation conditions. Instead, only occasional cases of mild secondary salinization have been reported, characterized by an increase in salt content from 1.63 to 2.85 g kg^{-1} over a 20-year period, which do not compromise overall system productivity (73). The marginal occurrence of "Good" soils and the absence of "Optimal" conditions suggest that improvements related to agricultural management are expressed within an intermediate functional range.

Although the SQIw revealed coherent spatial patterns, the coefficient of determination (R^2 = 0.246) reflects the inherent complexity of modeling composite indices in anthropogenically disturbed soils under a regional sampling density (approximately one sample per 3.5 ha). This limitation does not indicate model failure, but rather a scale mismatch as described by (50), whereby sharp chemical gradients associated with localized irrigation dynamics occur at distances smaller than the sampling interval, being inevitably incorporated into the residual error (nugget effect) and

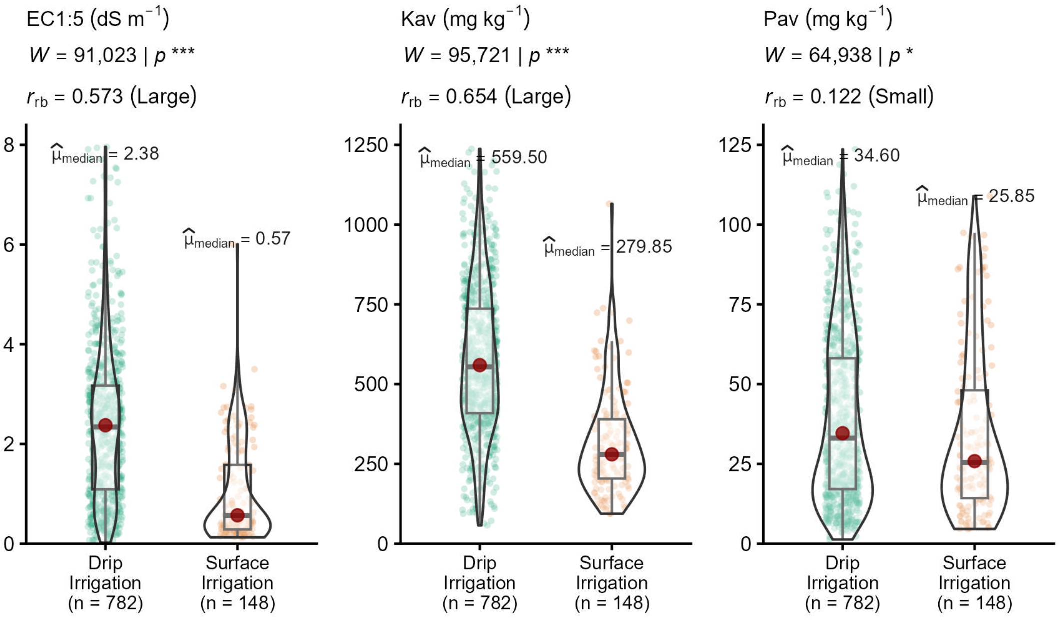

FIGURE 6
Effect of irrigation system on soil salinity and macronutrient availability. Combined violin and boxplots illustrate the distribution of EC1:5, Kav, and Pav under drip (n = 782) and surface irrigation (n = 148) systems. The central line and red dot represent the median, box edges indicate the interquartile range (25th–75th percentiles), and whiskers extend to 1.5 x IQR; individual observations are shown as jittered points. Statistical significance is based on the Mann-Whitney U test; r_{rb} denotes the rank-biserial correlation as a measure of effect size. the Y-axis scale were adjusted per variable to enhance the visualization of central tendency; statistical analysis included all observations.

thus constraining the R^2 value. Consistent with (74), the high local variability of variables such as electrical conductivity (EC) introduces stochastic noise that reduces point-scale accuracy, even though the model is able to filter these fluctuations and adequately represent regional-scale trends.

Despite these limitations in point-scale prediction, the low global bias of the model (Mean Error close to zero) supports the usefulness of the SQIw map for territorial planning. Consequently, the SQIw retains its value as a comparative diagnostic tool for identifying spatial gradients of soil quality and delineating zones for differentiated management.

4.4 Evolution of edaphic properties in Santa Rita

The earliest systematic records available for the Santa Rita de Siguas irrigation scheme date back to 1974, when the agricultural area covered approximately 1,492 ha. At that time, 83.5% of the area was classified as non-saline, with ECe values below 4 dS m^{-1}, whereas the remaining 16.5% exhibited moderate to strong salinity, with average salt concentrations ranging from 10 to 30 dS m^{-1}. A representative soil from the consolidated agricultural area showed a sandy loam to loamy sand texture, a slightly alkaline pH of 7.7, low soil organic matter content (1.8%), low surface salinity (ECe = 1.5 dS m^{-1}), and low exchangeable sodium, with an exchangeable sodium percentage (ESP) of 5.2% (21).

Complementarily, a study conducted in 1975 in a sector adjacent to the northeastern boundary of the irrigation scheme, an area that has not been incorporated into agriculture to date, described soils under initial conditions characterized by high surface salinity, and ECe values ranging from 4.8 to 75 dS m^{-1}. These soils exhibited very low available phosphorus (Pav; 0.8–3 mg kg^{-1}), high available potassium (Kav; 393–1,564 mg kg^{-1}), moderately alkaline pH values (7.2–7.8), and very low soil organic matter contents (0.1–0.2%). The assessments were conducted by pedological horizons down to approximately 10–40 cm depth and lacked precise spatial georeferencing (75). These values provide a reference for the pre-agricultural edaphic status of areas adjacent to the irrigation scheme.

At present, the agricultural area has expanded to approximately 3,200 ha. Results based on 930 composite samples collected at 0–20 cm depth indicate mean EC1:5 of 2.37 dS m^{-1}, with a range from 0.02 to 23.70 dS m^{-1}. When converted to ECe using the texture-specific pedotransfer function of (31), which explicitly incorporates individual sand and clay contents per sample (Supplementary Method S1; Equation 1), the mean EC1:5 of 2.37 dS m^{-1} corresponds approximately to a mean ECe of 24.08 dS m^{-1}, with a range of 0.21 to 246.80 dS m^{-1} (Supplementary Table 2). It is important to note that these values reflect the strongly skewed distribution of salinity across the irrigation scheme (CV = 87%, skewness = 2.79) rather than a uniform state of severe degradation. In this regard, the spatial distribution shown in Figure 4a and Supplementary Table 1 demonstrates that 93.86% of the mapped area presents EC1:5 values below 4.0 dS m^{-1}, with only 0.23% exceeding 8.0 dS m^{-1}. The extreme upper values that drive the statistical mean upward correspond to spatially restricted hotspots associated with parcels under poor salinity management and inadequate leaching fractions, where salt accumulation has progressed under active cultivation. This is consistent with the pre-agricultural conditions documented in adjacent areas in 1975, where ECe values reached up to 75 dS m^{-1}

(75), and with the findings of this study regarding the salinization risk under drip irrigation without adequate leaching. Furthermore, the dominance of salt-tolerant species such as *Opuntia ficus-indica*, which accounted for approximately 40% of the sampled sites, partially explains the persistence of productive activity under elevated salinity conditions. The applicability of the (31) model was confirmed by verifying that the textural properties of the study area fall within the model's calibration range (sand 3.6–84.6%; clay 7.4–48.5%), and the uncertainty propagation analysis confirmed that texture-induced variability does not alter the salinity classification of the delineated zones (Supplementary Figure 1). Although the (31) model is applicable within the textural range of the study area, its reliability may vary depending on soil conditions and requires validation in different regions, as acknowledged by the authors. Consequently, the converted ECe values should be interpreted as an approximation, and local validation using saturation extract measurements is recommended. In addition, mean available phosphorus (Pav) content was 48.59 mg kg^{-1} (1.30–990.10 mg kg^{-1}), available potassium (Kav) was 538.12 mg kg^{-1} (57.20–1,663.70 mg kg^{-1}), organic matter (OM) was 1.19% (0.30–8.50%) and soil pH averaged 7.49 (4.80–8.60).

The historical records from 1974 and 1975 provide important contextual information regarding the initial edaphic conditions of the irrigation scheme and adjacent areas prior to large-scale agricultural expansion. However, a direct quantitative comparison between these historical ECe values and the EC1:5 measurements obtained in the present study is not methodologically appropriate due to differences in analytical approaches. Instead, these data are better interpreted as evidence of the progressive spatial expansion of agriculture into inherently saline soils, which contributes to the pronounced spatial heterogeneity observed in current salinity patterns. In this context, variations in soil properties reflect the interaction between initial edaphic conditions and subsequent management practices under irrigation.

This pattern is consistent with practical evidence of intensive soil management in newly incorporated areas of the region. In these areas, high-capital interventions have enabled reductions in saturated soil extract electrical conductivity (ECe) from 44.8 to 3.84 dS m^{-1} and pH from 8.2 to 8.0 within the upper 30 cm of soil in only seven months. These results were accompanied by increases in available phosphorus from 10.5 to 124.0 mg kg^{-1} and soil organic matter from 0.14% to 2.47% (76). Although such management practices are not representative of the average farmer, they illustrate the edaphic mechanisms underlying the evolution observed under prolonged agricultural use in Santa Rita de Siguas.

4.5 Paradox of water-use efficiency: How drip irrigation can intensify soil salinity

The higher salinity levels observed under drip irrigation compared with surface irrigation cannot be attributed to differences in irrigation water quality, as both systems use the same water source. Rather, this pattern likely reflects the differences in salt redistribution dynamics associated with irrigation systems and their management conditions. In the study area, surface irrigation does not represent a homogeneous practice but varies according to crop type and rotation stage, including furrow irrigation for row crops and flood or border irrigation for alfalfa. These differences result in broader and more variable soil wetting patterns compared to drip irrigation. According to (77), in localized irrigation systems salts tend to accumulate at the soil surface and along the margins of the wetted bulb when an adequate leaching fraction is not applied, whereas under surface irrigation the larger irrigation depths promote deep leaching of salts beyond the root zone (78). demonstrated that radial water flow under drip irrigation promotes the progressive concentration of salts at the periphery of the wetted front, particularly under high evaporation rates typical of arid climates. Likewise (79), noted that when leaching requirements are not met, soil salinity can increase even under highly efficient irrigation systems such as drip irrigation.

The higher concentrations of available phosphorus (Pav) and potassium (Kav) observed in soils under drip irrigation may result from the combined effects of the intrinsically low mobility of these nutrients and irrigation management practices. Phosphorus is rapidly immobilized through adsorption and precipitation with Fe–Al oxides and Ca, whereas K^+ is retained at cation exchange sites and fixed within 2:1 clay minerals, thereby limiting its vertical movement (80, 81). Drip irrigation may further restrict nutrient displacement by confining water distribution to a limited soil volume near the surface, minimizing deep percolation and concentrating solute transport within the root zone (82, 83). The frequent and split application of water and fertilizers through fertigation (84, 85) may promote the gradual accumulation of applied nutrients within the wetted bulb, as effective leaching events are seldom practiced in the study area.

Additionally, in the study area, a substantial proportion of drip-irrigated fields correspond to recently incorporated agricultural land. In these areas, the same water allocation is used to irrigate larger surface areas than under surface irrigation. This strategy, aimed at maximizing water-use efficiency, generally involves the application of reduced irrigation depths without an adequate leaching fraction. As a consequence, the leaching of pre-existing salts in inherently saline soils is limited, promoting their progressive accumulation, together with low-mobility nutrients, within the wetted bulb. In this context, drip irrigation, when not accompanied by appropriate salinity management, may intensify solute concentration processes and increase the risk of secondary soil salinization.

Although waterlogging and capillary-driven salinization could theoretically contribute to salt accumulation in irrigated arid soils, these processes are unlikely to represent dominant mechanisms in the Santa Rita de Siguas irrigation scheme. As described in Section 2.1, the scheme is established on a high alluvial plain adjacent to the Siguas River valley, whose floor lies approximately 200 m lower in elevation, a pronounced topographic gradient that likely favors natural lateral subsurface drainage. No formal artificial drainage infrastructure was identified in the sampled parcels during field work. Under these conditions, the secondary salinization observed is more likely associated with insufficient leaching fractions than with waterlogging processes, consistent with salt accumulation mechanisms described for arid irrigated soils without adequate leaching (52, 77). Nevertheless, the absence of formal water table monitoring data is acknowledged as a limitation, and future studies should explicitly characterize the subsurface hydraulic conditions of the scheme.

As noted above, however, this context itself introduces an important confounding factor that must be explicitly acknowledged. Drip-irrigated fields in the study area correspond predominantly to recently incorporated agricultural land, while surface-irrigated fields represent older, more consolidated areas with longer histories of organic matter inputs, fertilization, and salt management. Consequently, differences in EC, Kav, and Pav between irrigation systems may reflect the combined effect of irrigation method, land development age, crop type, and management intensity rather than the isolated effect of the irrigation system alone. The comparison should therefore be interpreted as associative rather than causal, and controlled experimental designs are needed to isolate the specific contribution of each irrigation system to soil salinity and nutrient dynamics.

4.6 Implications for management and sustainability

In areas classified as "Poor", the variables with the greatest weight in the index equation (sand, EC1:5, available potassium (Kav) and OM) exhibited limited values, characterized by sandy texture EC1:5 levels reaching up to 23.70 dS m^{-1} and low contents of OM and Kav. These conditions may synergistically constrain agricultural productivity (86). Sustainable recovery requires integrated management strategies, including salt leaching combined with improved subsurface drainage to reduce soil electrical conductivity to tolerable thresholds (76, 87). In addition, the incorporation of organic amendments could enhance soil structure, CEC and water retention in sandy soils (88, 89), while balanced potassium fertilization is required to overcome nutritional constraints (90).

Additionally, phytoremediation using halophytic species may be adopted, as it shows potential as a low water-input management strategy; however, its effectiveness still requires validation at the field scale (91). Complementarily, the adoption of salt-tolerant crops represents a key adaptation strategy for soils that have been recently incorporated into agricultural production or degraded by improper management practices. In the study area, some farmers have successfully introduced prickly pear (*Opuntia ficus-indica*), a species well adapted to the saline, water-limited, and nutrient-poor stress conditions that characterize these edaphic environments, thereby demonstrating the productive viability of resilient agricultural systems under restrictive conditions (92, 93).

Soils classified as "Acceptable" SQIw represent transitional systems in which management practices have contributed to improving initial soil conditions. However, these soils remain vulnerable to adverse effects derived from agricultural management; under these conditions, system sustainability depends on the implementation of preventive strategies grounded in soil quality assessment. These strategies include the optimization of tillage and irrigation practices, salinity monitoring, and balanced nutrient management, particularly potassium, to maintain soil fertility and prevent degradation processes such as secondary salinization or excessive nutrient accumulation (60, 94). The implementation of these practices is critical for stabilizing soil quality and preventing its transition toward lower SQIw classes.

Overall, SQIw-based zonification highlights that sustainability in irrigated systems within arid regions strongly depends on the appropriate alignment between management intensity and the soil's functional capacity. This dependence is particularly related to resilience against physical, chemical, and biological degradation processes. By integrating the indirect effects of irrigation practices through measurable edaphic properties, the SQIw framework provides a scientifically robust basis for adaptive management. This approach is aimed at minimizing salinity risks, enhancing soil resilience, and sustaining long-term agricultural productivity under conditions of limited water availability (53, 88).

4.7 Global applicability and transferability of the proposed methodology

Despite the use of a reduced set of indicators, the proposed methodological approach demonstrates high transferability to other irrigated arid and semi-arid agroecosystems, where the detailed soil information is often limited. The integration of routinely measured chemical properties and textural information enables regional-scale spatial assessments of soil quality without complex analyses or long-term monitoring, as reported in previous studies on integrated soil quality evaluation in arid environments (1, 95). Although electrical conductivity was determined using a 1:5 soil-to-water ratio rather than the saturated paste extract (ECe), this approach remains suitable for comparative spatial analyses in regional studies, provided that its limitations for estimating leaching requirements are acknowledged (64).

Nevertheless, the SQI results should be interpreted in light of several methodological limitations. Parcel selection based on voluntary farmer participation may introduce self-selection bias, as participating farmers could differ systematically from non-participants in management practices, crop type, and land quality. The absence of sodicity indicators, such as the sodium adsorption ratio (SAR) or exchangeable sodium percentage (ESP), along with the lack of soluble anions and cations data, constrains a comprehensive assessment of soil structural risk and leaching requirements. Sampling restricted to the upper 20 cm of the soil profile may underestimate salt accumulation and redistribution at greater depths under different irrigation systems. The exclusion of biological indicators and key physical properties, such as bulk density and infiltration rate, further limits the interpretation of soil functionality from an ecosystem-based perspective. The Kav scoring function was anchored to the observed dataset range following (32), which maximizes local discrimination but does not directly reflect crop-specific sufficiency standards for the dominant species in the scheme. The comparison between irrigation systems is also potentially confounded by differences in land development age, crop history, and management intensity, which were not controlled for in the study design. Finally, the discrepancy between point-based sample statistics and kriged areal class proportions should be interpreted with caution, as both representations operate at different spatial supports and are not directly comparable.

Future research should incorporate probabilistic or stratified sampling designs, depth-stratified sampling, sodicity indicators and soluble fractions, selected physical and biological variables, and locally validated agronomic thresholds for potassium availability.

These refinements would strengthen the mechanistic interpretation of the SQI and enhance its applicability for sustainable soil management in irrigated arid regions.

5 Conclusions

This study demonstrates that, under arid and naturally saline soil conditions in Santa Rita de Siguas, the adoption of drip irrigation without an adequate leaching fraction is associated with increased soil salinity. In addition, nutrient accumulation is enhanced under these conditions. These findings challenge the notion that improved water-use efficiency invariably leads to better soil quality.

The weighted and spatially explicit Soil Quality Index developed in this study effectively characterized regional gradients of soil quality under irrigation. The results revealed a landscape dominated by intermediate soil quality classes, with no evidence of extreme degradation or optimal edaphic conditions. This pattern indicates a partial improvement relative to the initial saline conditions. However, it also highlights the persistence of inherent soil constraints that limit soil recovery through conventional management practices.

Overall, the proposed methodological framework, based on routine soil analyses and geostatistical tools, demonstrated high transferability to other irrigation schemes in arid regions. It provides key spatial information to support site-specific management, the prioritization of critical areas, and the optimization of irrigation and fertilization practices. Future studies should incorporate sodicity indicators, extend the sampling depth, and integrate soil physical and biological properties. These improvements would enable a more comprehensive assessment of soil quality and strengthen the long-term sustainability of agricultural systems in arid and semi-arid regions.

Data availability statement

The original contributions presented in the study are included in the article/Supplementary Material. Further inquiries can be directed to the corresponding author.

Author contributions

RP-C: Writing – review & editing, Writing – original draft, Methodology, Conceptualization, Investigation. CV-G: Writing – review & editing, Software, Formal analysis, Writing – original draft, Visualization. EC-M: Writing – original draft. PG-C: Writing – original draft.

Funding

The author(s) declared that financial support was received for this work and/or its publication. The work was funded by the INIA project CUI 2487112 "Mejoramiento de los servicios de investigación y transferencia tecnológica en el manejo y recuperación de suelos agrícolas degradados y aguas para riego en la pequeña y mediana agricultura en los departamentos de Lima, Áncash, San Martín, Cajamarca, Lambayeque, Junín, Ayacucho, Arequipa, Puno y Ucayali".

Acknowledgments

We also thank the technical staff of the Laboratorio de Suelos, Aguas y Foliares (LABSAF) for carrying out the complete laboratory work, from sample preparation to analysis, and the field teams for their dedicated work during the sampling campaign. Special thanks are extended to the Junta de Usuarios Santa Rita de Siguas for granting access to their agricultural fields and sharing valuable agronomic information.

Conflict of interest

The author(s) declared that this work was conducted in the absence of any commercial or financial relationships that could be construed as a potential conflict of interest.

Generative AI statement

The author(s) declared that generative AI was not used in the creation of this manuscript.

Any alternative text (alt text) provided alongside figures in this article has been generated by Frontiers with the support of artificial intelligence and reasonable efforts have been made to ensure accuracy, including review by the authors wherever possible. If you identify any issues, please contact us.

Publisher's note

Supplementary material

The Supplementary Material for this article can be found online at: https://www.frontiersin.org/articles/10.3389/fsoil.2026.1789869/full#supplementary-material

References

1. Andrews SS, Karlen DL, Cambardella CA. The soil management assessment framework: A quantitative soil quality evaluation method. *Soil Sci Soc Am J*. (2004) 68:1945–62. doi: 10.2136/sssaj2004.1945

2. Karlen DL, Andrews SS, Weinhold BJ, Doran JW. Soil quality: Humankind's foundation for survival. *J Soil Water Conserv*. (2003) 58:171–9. doi: 10.1080/00224561.2003.12457524

3. Qi Y, Darilek JL, Huang B, Zhao Y, Sun W, Gu Z. Evaluating soil quality indices in an agricultural region of Jiangsu Province, China. *Geoderma*. (2009) 149:325–34. doi: 10.1016/j.geoderma.2008.12.015

4. Jordán MM, Navarro-Pedreño J, García-Sánchez E, Mateu J, Juan P. Spatial dynamics of soil salinity under arid and semi-arid conditions: Geological and environmental implications. *Environ Geol*. (2004) 45:448–56. doi: 10.1007/s00254-003-0894-y

5. Cemek B, Güler M, Kiliç K, Demir Y, Arslan H. Assessment of spatial variability in some soil properties as related to soil salinity and alkalinity in Bafra plain in northern Turkey. *Environ Monit Assess*. (2007) 124:223–34. doi: 10.1007/s10661-006-9220-y

6. Sun G, Zhu Y, Gao Z, Yang J, Qu Z, Mao W, et al. Spatiotemporal patterns and key driving factors of soil salinity in dry and wet years in an arid agricultural area with shallow groundwater table. *Agriculture*. (2022) 12:1243. doi: 10.3390/agriculture12081243

7. Bünemann EK, Bongiorno G, Bai Z, Creamer RE, De Deyn G, De Goede R, et al. Soil quality – A critical review. *Soil Biol Biochem*. (2018) 120:105–25. doi: 10.1016/j.soilbio.2018.01.030

8. Elbasiouny H, Elbehiry F, Abowaly M. Soil quality indices - Special focus on salt-affected soil: Review and case study in Northern Egypt. *Environment Biodiversity Soil Secur*. (2017) 1:85–100. doi: 10.21608/jenvbs.2017.1085.1005

9. Farag AA, El-Aziz MAA, El-Husseiny A. Effects of irrigation systems and water management strategies on soil chemical properties and citrus tree productivity in clayey soils. *Sci Rep*. (2025) 15:33324. doi: 10.1038/s41598-025-19575-6

10. Phocaides A. *Handbook on pressurized irrigation techniques*. Rome: FAO (2007).

11. Du Y, Liu X, Zhang L, Zhou W. Drip irrigation in agricultural saline-alkali land controls soil salinity and improves crop yield: Evidence from a global meta-analysis. *Sci Total Environ*. (2023) 880:163226. doi: 10.1016/j.scitotenv.2023.163226

12. Zaman M, Shahid SA, Heng L. Irrigation systems and zones of salinity development. In: *Guideline for Salinity Assessment, Mitigation and Adaptation Using Nuclear and Related Techniques*. Springer International Publishing, Cham (2018). p. 91–111. doi: 10.1007/978-3-319-96190-3_4

13. Sharma KL, Mandal UK, Srinivas K, Vittal KPR, Mandal B, Grace JK, et al. Long-term soil management effects on crop yields and soil quality in a dryland Alfisol. *Soil Tillage Res*. (2005) 83:246–59. doi: 10.1016/j.still.2004.08.002

14. Fernández MP, Keshavarzi A, Rodrigo-Comino J, Schnabel S, Contador JFL, Gutiérrez ÁG, et al. Developing scoring functions to assess soil quality at a regional scale in rangelands of SW Spain. *Rev Bras Ciec do Solo*. (2020) 44:e0200090. doi: 10.36783/18069657rbcs20200090

15. Abdel-Fattah MK, Mohamed ES, Wagdi EM, Shahin SA, Aldosari AA, Lasaponara R, et al. Quantitative evaluation of soil quality using principal component analysis: The case study of El-Fayoum Depression Egypt. *Sustainability*. (2021) 13:1824. doi: 10.3390/su13041824

16. Villarroel JS, Martinez RVC. Característica fisicoquímica de suelos salinos agrícolas en el Fundo Tercer Mundo - Cañete. *Rev Investigación Cañetana*. (2025) 3:66–76. doi: 10.60091/ric.2024.v3n2.02

17. Zong R, Wang Z, Li W, Li H, Ayantobo OO. Effects of practicing long-term mulched drip irrigation on soil quality in Northwest China. *Sci Total Environ*. (2023) 878:163247. doi: 10.1016/j.scitotenv.2023.163247

18. Zhang L, Chang Y, Gao W, Li X, Jiang H, Zhou R, et al. Assessment of the quality indices of soils irrigated by groundwater in a typical semi-arid steppe ecoregion. *Pol J Environ Stud*. (2022) 31:1951–61. doi: 10.15244/pjoes/143302

19. Bijarnia SL, Singh R, Godara AS, Jakhar RK, Meena D, Damor K, et al. Evaluation of salinity, sodicity and fertility indices of soils of south-eastern Jodhpur (Rajasthan), India. *J Soil Salinity Water Qual*. (2025) 17:35–43. doi: 10.56093/jsswq.v17i1.166633

20. Yang F, Zhang G, Yin X, Liu Z. Field-scale spatial variation of saline-sodic soil and its relation with environmental factors in Western Songnen Plain of China. *Int J Environ Res Public Health*. (2011) 8:374–87. doi: 10.3390/ijerph8020374

21. Oficina Nacional de Evaluación de Recursos Naturales (ONERN). *Inventario, evaluación y uso racional de los recursos naturales de la costa: cuencas de los ríos Quilca y Tambo* (1974). Available online at: https://hdl.handle.net/20.500.12543/231 (Accessed October 12, 2025).

22. Ministerio de Desarrollo Agrario y Riego del Perú (MIDAGRI). *Superficie agrícola del Perú* (2024). Available online at: https://siea.midagri.gob.pe/portal/informativos/superficie-agricola-peruana (Accessed October 10, 2025).

23. Servicio Nacional de Meteorología e Hidrología del Perú (SENAMHI). *Descarga de datos meteorológicos*. Available online at: https://www.senamhi.gob.pe/site/descarga-datos/ (Accessed October 10, 2025).

24. Abate GG. Soil sampling and sample preparation. *Int J Modern Sci Res Technol*. (2025) 3:167–76. doi: 10.5281/zenodo.14810773

25. Tan KH. *Soil sampling, preparation, and analysis*. Boca Raton, FL: Taylor & Francis (2005). p. 672.

26. International Organization for Standardization - ISO. *Soil quality —Pretreatment of samples for physico-chemical analysis (ISO 11464:2006)*. Geneva, Switzerland: ISO (2006). Available online at: https://www.iso.org/standard/37718.html (Accessed January 15, 2025).

27. Secretaría de Medio Ambiente y Recursos Naturales - SEMARNAT. *NORMA Oficial Mexicana NOM-021-RECNAT-2000, Que establece las especificaciones de fertilidad, salinidad y clasificación de suelos. Estudios, muestreo y análisis* (2002). Available online at: https://www.ordenjuridico.gob.mx/Documentos/Federal/wo69255.pdf (Accessed January 15, 2025).

28. United States Environmental Protection Agency - US EPA. *Method 9045D: Soil and waste pH*. Washington, D.C. USA: US EPA (2004). Available online at: https://www.epa.gov/sites/default/files/2015-12/documents/9045d.pdf (Accessed January 15, 2025).

29. International Organization for Standardization - ISO. *Soil quality —Determination of the specific electrical conductivity (ISO 11265:1994)*. Geneva, Switzerland: ISO (1994). Available online at: https://www.iso.org/standard/19243.html (Accessed January 15, 2025).

30. Soil Science Division Staff. *Soil survey manual*. Ditzler C, Scheffe K, Monger HC, editors. Washington, D.C: Government Printing Office (2017). USDA Handbook.

31. Kargas G, Londra P, Sotirakoglou K. The effect of soil texture on the conversion factor of 1:5 soil/water extract electrical conductivity (EC1:5) to soil saturated paste extract electrical conductivity (ECe). *Water*. (2022) 14:642. doi: 10.3390/w14040642

32. Maleki S, Zeraatpisheh M, Karimi A, Sareban G, Wang L. Assessing variation of soil quality in agroecosystem in an arid environment using digital soil mapping. *Agronomy*. (2022) 12:578. doi: 10.3390/agronomy12030578

33. Andrews SS, Karlen DL, Mitchell JP. A comparison of soil quality indexing methods for vegetable production systems in Northern California. *Agric Ecosyst Environ*. (2002) 90:25–45. doi: 10.1016/S0167-8809(01)00174-8

34. Ghimire P, Shrestha S, Acharya A, Wagle A, Acharya TD. Soil fertility mapping of a cultivated area in Resunga Municipality, Gulmi, Nepal. *PloS One*. (2024) 19:e0292181. doi: 10.1371/journal.pone.0292181

35. Moran PAP. Notes on continuous stochastic phenomena. *Biometrika*. (1950) 37:17–23. doi: 10.2307/2332142

36. Cliff AD, Ord JK. *Spatial processes: models & applications*. London: Pion Limited (1981) 266.

37. Cambardella CA, Moorman TB, Novak JM, Parkin TB, Karlen DL, Turco RF, et al. Field-scale variability of soil properties in Central Iowa soils. *Soil Sci Soc Am J*. (1994) 58:1501–11. doi: 10.2136/sssaj1994.03615995005800050033x

38. Yamamoto JK. On unbiased backtransform of lognormal kriging estimates. *Comput Geosci*. (2007) 11:219–34. doi: 10.1007/s10596-007-9046-x

39. QGIS Development Team. *QGIS geographic information system*. QGIS Association (2025). Available online at: https://www.qgis.org (Accessed November 16, 2025).

40. Kerby DS. The simple difference formula: An approach to teaching nonparametric correlation1. *Compr Psychol*. (2014) 3:11.IT.3.1. doi: 10.2466/11.IT.3.1

41. Cohen J. *Statistical power analysis for the behavioral sciences*. Hillsdale, N.J: L. Erlbaum Associates (1988). p. 567.

42. R Core Team. *R: A language and environment for statistical computing*. Vienna, Austria: R Foundation for Statistical Computing (2024). Available online at: https://www.R-project.org/ (Accessed December 12, 2025).

43. Revelle W. *psych: Procedures for psychological, psychometric, and personality research*. Evanston, Illinois: Northwestern University (2025). Available online at: https://CRAN.R-project.org/package=psych (Accessed December 12, 2025).

44. Wei T, Simko V. *R package "corrplot": Visualization of a correlation matrix* (2024). Available online at: https://github.com/taiyun/corrplot (Accessed January 7, 2026).

45. Lê S, Josse J, Husson F. FactoMineR: An R package for multivariate analysis. *J Stat Software*. (2008) 25(1):1–18. doi: 10.18637/jss.v025.i01

46. Bivand RS, Wong DWS. Comparing implementations of global and local indicators of spatial association. *Test*. (2018) 27:716–48. doi: 10.1007/s11749-018-0599-x

47. Pebesma EJ. Multivariable geostatistics in S: The gstat package. *Comput Geosciences*. (2004) 30:683–91. doi: 10.1016/j.cageo.2004.03.012

48. Ben-Shachar MS, Lüdecke D, Makowski D. effectsize: Estimation of effect size indices and standardized parameters. *J Open Source Software*. (2020) 5:2815. doi: 10.21105/joss.02815

49. Patil I. Visualizations with statistical details: The "ggstatsplot" approach. *J Open Source Software*. (2021) 6:3167. doi: 10.21105/joss.03167

50. Webster R, Oliver MA. *Geostatistics for Environmental Scientists*. Chichester: John Wiley & Sons, Ltd (2007). doi: 10.1002/9780470517277

51. Weil RR, Brady NC. *The nature and properties of soils*. Columbus: Pearson (2017) p. 1–1086.

52. Richards LA. Diagnosis and improvement of saline and alkali soils. *Soil Sci*. (1954) 78:154. doi: 10.1097/00010694-195408000-00012

53. Qadir M, Oster JD, Schubert S, Noble AD, Sahrawat KL. "Phytoremediation of sodic and saline-sodic soils." In: *Advances in Agronomy*. Amsterdam: Academic Press (2007). p. 197–247. doi: 10.1016/S0065-2113(07)96006-X

54. Schlesinger WH. Carbon storage in the caliche of arid soils: a case study from Arizona. *Soil Sci*. (1982) 133:247–55. doi: 10.1097/00010694-198204000-00008

55. Lal R. Soil carbon sequestration impacts on global climate change and food security. *Science*. (2004) 304:1623–7. doi: 10.1126/science.1097396

56. Fixen PE, Grove JH. "Testing soils for phosphorus." In: Westerman RL, editor. *SSSA Book Series 1st ed*. Madison: Soil Science Society of America (1990). p. 141–80. doi: 10.2136/sssabookser3.3ed.c7

57. Hinsinger P. Bioavailability of soil inorganic P in the rhizosphere as affected by root-induced chemical changes: a review. *Plant Soil*. (2001) 237:173–95. doi: 10.1023/A:1013351617532

58. Penn C, Camberato J. A critical review on soil chemical processes that control how soil pH affects phosphorus availability to plants. *Agriculture*. (2019) 9:120. doi: 10.3390/agriculture9060120

59. Sparks DL, Huang PM. "Physical chemistry of soil potassium." In: Munson RD, editor.*ASA, CSSA, and SSSA Books 1st ed*. Madison: American Society of Agronomy, Crop Science Society of America, Soil Science Society of America (1985). p. 201–76. doi: 10.2134/1985.potassium.c9

60. Zörb C, Senbayram M, Peiter E. Potassium in agriculture – status and perspectives. *J Plant Physiol*. (2014) 171:656–69. doi: 10.1016/j.jplph.2013.08.008

61. Dexter AR. Soil physical quality. *Geoderma*. (2004) 120:201–14. doi: 10.1016/j.geoderma.2003.09.004

62. Poudel D, Abiye W, Dengiz O, Pacci S, Saflı ME. Soil quality dynamics in natural pine forests lands integrating fuzzy-AHP and prediction based on random forest algorithms. *Sci Rep*. (2025) 15:38012. doi: 10.1038/s41598-025-21943-1

63. Parra-González S, Rodriguez-Valenzuela J. Determination of the soil quality index by principal component analysis in cocoa agroforestry system in the Orinoco region, Colombia. *J Agric Ecol Res Int*. (2017) 10:1–8. doi: 10.9734/JAERI/2017/31346

64. Nabiollahi K, Taghizadeh-Mehrjardi R, Kerry R, Moradian S. Assessment of soil quality indices for salt-affected agricultural land in Kurdistan Province, Iran. *Ecol Indic*. (2017) 83:482–94. doi: 10.1016/j.ecolind.2017.08.001

65. Corwin DL, Lesch SM. Apparent soil electrical conductivity measurements in agriculture. *Comput Electron Agric*. (2005) 46:11–43. doi: 10.1016/j.compag.2004.10.005

66. Johnston AE, Poulton PR, Fixen PE, Curtin D. "Phosphorus: its efficient use in agriculture." In: *Advances in Agronomy*. San Diego: Academic Press (2014). p. 177–228. doi: 10.1016/B978-0-12-420225-2.00005-4

67. Karlen DL, Mausbach MJ, Doran JW, Cline RG, Harris RF, Schuman GE. Soil quality: a concept, definition, and framework for evaluation (a guest editorial). *Soil Sci Soc Am J*. (1997) 61:4–10. doi: 10.2136/sssaj1997.03615995006100010001x

68. Conceição PC, Amado TJC, Mielniczuk J, Spagnollo E. Soil organic matter and other attributes as indicators to evaluate soil quality in conservation systems. *Rev Bras Ciec do Solo*. (2005) 29:777–88. doi: 10.1590/S0100-06832005000500013

69. Santos FCD, Albuquerque Filho MRD, Soares JR, Jesmin T, Manirakiza N, Silveira MCTD, et al. Organic matter: a critical soil health indicator in agrosystems within the Cerrado of Bahia, Brazil and South Florida, USA. *Front Soil Sci*. (2025) 5:1524550. doi: 10.3389/fsoil.2025.1524550

70. Gao J, Zhang J, Gong Y, Yang K, Quan W, Li L, et al. A robust soil quality index for mountain ecosystems driven by XGBoost and network analysis. *Geoderma*. (2025) 463:117558. doi: 10.1016/j.geoderma.2025.117558

71. Romaniuk R, Giuffré L, Costantini A, Bartoloni N, Nannipieri P. A comparison of indexing methods to evaluate quality of soils: the role of soil microbiological properties. *Soil Res*. (2012) 49:733–41. doi: 10.1071/SR11147

72. Andrews SS, Mitchell JP, Mancinelli R, Karlen DL, Hartz TK, Horwath WR, et al. On-farm assessment of soil quality in California's Central Valley. *Agron J*. (2002) 94:12–23. doi: 10.2134/agronj2002.1200

73. Liu S, Li F, Zhang Q, Li Z, Tian C, Qiao Y, et al. Soil quality improvement with increasing reclamation years in the Yellow River Delta. *Agronomy*. (2023) 13:2576. doi: 10.3390/agronomy13102576

74. Angelini ME, Heuvelink GBM, Lagacherie P. A multivariate approach for mapping a soil quality index and its uncertainty in southern France. *Eur J Soil Sci*. (2023) 74: e13345. doi: 10.1111/ejss.13345

75. Ministerio de Agricultura Dirección General de Aguas Dirección de Preservación y Conservación. *Estudio agrológico detallado de las pampas de Majes y Siguas: departamento de Arequipa*. Lima: Ministerio de Agricultura. (1975). Available online at: https://repositorio.ana.gob.pe/item/8301a1ad-d1e6-4b49-bad4-d6e011460bdd (Accessed October 12, 2025).

76. Tixe Pérez GS. *Manejo de salinidad en la instalación de cultivos de exportación en Santa Rita de Siguas*. Lima (PE: Universidad Nacional Agraria La Molina (2023). Bachelor's thesis.

77. Ayers RS, Westcot DW. *Water quality for agriculture*. Rome: Food and Agriculture Organization of the United Nations (1985) p. 1–174. FAO irrigation and drainage paper.

78. Bresler E. "Trickle-drip irrigation: principles and application to soil-water management." In: *Advances in Agronomy*. New York: Academic Press (1977). p. 343–93. doi: 10.1016/S0065-2113(08)60222-9

79. Letey J, Hoffman GJ, Hopmans JW, Grattan SR, Suarez D, Corwin DL, et al. Evaluation of soil salinity leaching requirement guidelines. *Agric Water Manage*. (2011) 98:502–6. doi: 10.1016/j.agwat.2010.08.009

80. Sparks DL. Potassium dynamics in soils. In: Stewart BA, editor.*Advances in Soil Science*. Springer New York, New York, NY (1987). p. 1–63. Advances in Soil Science; vol. 6. doi: 10.1007/978-1-4612-4682-4_1

81. Havlin J. *Soil fertility and fertilizers: an introduction to nutrient management*. Upper Saddle River, N.J: Pearson (2014) p. 1–516.

82. Hansona BR, Schwankl LJ, Schulbach KF, Pettygrove GS. A comparison of furrow, surface drip, and subsurface drip irrigation on lettuce yield and applied water. *Agric Water Manage*. (1997) 33:139–57. doi: 10.1016/S0378-3774(96)01289-9

83. Li Z, Zong R, Wang T, Wang Z, Zhang J. Adapting root distribution and improving water use efficiency via drip irrigation in a jujube (Zizyphus jujube Mill.) orchard after long-term flood irrigation. *Agriculture*. (2021) 11:1184. doi: 10.3390/agriculture11121184

84. Bar-Yosef B. "Advances in fertigation." In: *Advances in Agronomy*. San Diego: Academic Press (1999). p. 1–77. doi: 10.1016/S0065-2113(08)60910-4

85. Yang P, Wu L, Cheng M, Fan J, Li S, Wang H, et al. Review on drip irrigation: impact on crop yield, quality, and water productivity in China. *Water*. (2023) 15:1733. doi: 10.3390/w15091733

86. Qadir M, Quillérou E, Nangia V, Murtaza G, Singh M, Thomas RJ, et al. Economics of salt-induced land degradation and restoration. *Nat Resour Forum*. (2014) 38:282–95. doi: 10.1111/1477-8947.12054

87. Khoshgoftarmanesh AH, Shariatmadari H, Vakil R. Reclamation of saline soils by leaching and barley production. *Commun Soil Sci Plant Anal*. (2003) 34:2875–83. doi: 10.1081/CSS-120025198

88. Lal R. Restoring soil quality to mitigate soil degradation. *Sustainability*. (2015) 7:5875–95. doi: 10.3390/su7055875

89. Arriaga FJ, Lowery B. Soil physical properties and crop productivity of an eroded soil amended with cattle manure. *Soil Sci*. (2003) 168:888–99. doi: 10.1097/01.ss.0000106403.84926.7e

90. Rengasamy P. Soil processes affecting crop production in salt-affected soils. *Funct Plant Biol*. (2010) 37:613–20. doi: 10.1071/FP09249

91. Shankar V, Evelin H. Strategies for reclamation of saline soils. In: Giri B, Varma A, editors.*Microorganisms in Saline Environments: Strategies and Functions*. Springer International Publishing, Cham (2019). p. 439–49. Soil Biology; vol. 56. doi: 10.1007/978-3-030-18975-4_19

92. Zegbe JA, Servín-Palestina M. Supplemental irrigation to save water while growing cactus pear in semi-arid regions*. *Irrig Drain*. (2021) 70:269–80. doi: 10.1002/ird.2542

93. Gajender G, Singh G, Dagar JC, Lal K, Yadav RK. Performance of edible cactus (Opuntiaficus-indica) in saline environments. *Indian J Agric Sci*. (2014) 84(4):509–13. doi: 10.56093/ijas.v84i4.39469

94. Askari MS, Holden NM. Quantitative soil quality indexing of temperate arable management systems. *Soil Tillage Res*. (2015) 150:57–67. doi: 10.1016/j.still.2015.01.010

95. Nasir M, Haider M, Ali Z, Akhtar W, Alam S. Evaluation of soil quality through simple additive soil quality index (SQI) of Tehsil Charsadda, Khyber Pakhtunkhwa, Pakistan. *J Saudi Soc Agric Sci*. (2024) 23:42–54. doi: 10.1016/j.jssas.2023.09.001